Journal of Soils and Sediments (2021) 21:257–280
https://doi.org/10.1007/s11368-020-02764-3

SOILS, SEC 3 • REMEDIATION AND MANAGEMENT OF CONTAMINATED OR DEGRADED LANDS • RESEARCH ARTICLE

# Does calcium carbonate influence clay mineral transformation in soils developed from slope deposits in Southern Poland?

Joanna Beata Kowalska[1] · Michał Skiba[2] · Katarzyna Maj-Szeliga[2] · Ryszard Mazurek[3] · Tomasz Zaleski[3]

Received: 12 March 2020 / Accepted: 23 August 2020 / Published online: 1 September 2020


## Abstract

**Purpose** Literature reported that soils characterized by heterogeneity would reveal the different direction of clay minerals transformation. Hence, in this study, four soils developed on menilite shales slope deposits were investigated to test if the clay minerals transformations in soils with varied calcium carbonate distribution would show multidirectional paths of clay mineral weathering, or if transformation of secondary phases in such stratified materials would reveal only one trajectory.

**Methods** The separated clay fractions were analysed using X-ray diffractometry and Fourier-transform infrared spectroscopy. Geochemical analyses were performed using ICP-ES and ICP-MS after sample fusion with lithium borate and an alloy dissolution with nitric acid.

**Results** Calcium carbonate did not influence the composition and transformation of clay minerals. Despite the fact that soils were characterized by different content and distribution of calcium carbonate within the solum and additionally indicated various morphological features, the mineralogical composition of clay fraction was very uniform. Among the secondary phases, chlorite, illite, vermiculite, kaolinite and mixed phases illite-smectite and vermiculite-chlorite were detected in all horizons.

**Conclusions** The uniform composition of the clay minerals in the studied soils suggested that mass movement, which controlled the formation of slope covers, was probably of a similar character and intensity across the whole of the slope. Furthermore, it seems that the pedogenesis in all soils proceeded on the same scale of advancement. This was indicated by a similar degree of weathering of soil material and lack of depth-dependent weathering in the profiles, confirmed by values of weathering indices (CIA and ICV) as well as by micromorphologically visible, highly weathered coarse fragments. Moreover, weak intensity of the illuviation process within the homogeneous substrate could have resulted in the very uniform composition of clay minerals in the studied soils.

**Keywords** Mineral transformation · Sudoite · Dioctahedral vermiculite · Mixing soil material · Weathering indices

Responsible editor: Claudio Colombo

**Electronic supplementary material** The online version of this article (https://doi.org/10.1007/s11368-020-02764-3) contains supplementary material, which is available to authorized users.

✉ Michał Skiba
michal.skiba@uj.edu.pl

Joanna Beata Kowalska
joanna.kowalska@upwr.edu.pl

Katarzyna Maj-Szeliga
katarzyna.maj@uj.edu.pl

Tomasz Zaleski
tomasz.zaleski@urk.edu.pl

[1] Institute of Soil Science and Environmental Protection, Wroclaw University of Environmental and Life Sciences, ul. Grunwaldzka 53, 50-357 Wroclaw, Poland

[2] Institute of Geological Sciences, Jagiellonian University, ul. Gronostajowa 3a, 30-387 Kraków, Poland

[3] Department of Soil Science and Agrophysics, University of Agriculture, Al. Mickiewicza 21, 31-120 Kraków, Poland

## 1 Introduction

Clay minerals are important constituents of soils because they are very reactive and control many geochemical processes taking place in soils, such as element cycling, nutrient release and availability. Taking this into consideration, understanding of clay minerals weathering in soils appears to be an important issue. In general, four major processes controlling the clay mineralogy of soils can be distinguished: inheritance from pre-existing parent material, transformation of the inherited clay minerals, neoformation of clays via crystallization from soil solutions and aeolian deposition of allochthonous materials (Barton and Karathanasis 2002; Eberl et al. 1984; Velde and Meunier 2011; Waroszewski et al. 2016; Wilson 1999; Yousefifard et al. 2015).

Micas and most chlorites present in soils are inherited from parent rocks. They are formed at elevated pressure and temperature conditions during diagenetic, metamorphic and igneous processes. Because of this, they are unstable in the soil environment where they undergo weathering leading to formation of more stable phases. Micas in general are believed to transform into swelling phases—that is, vermiculite or smectite. However, the exact mechanisms of these transformations are not known in detail. Especially for dioctahedral mica, no clear picture of the transformation can be derived from the available literature. Most studies available (e.g. Churchman and Lowe 2012; Righi et al. 1999; Skiba 2007) report formation of dioctahedral vermiculite at the expense of dioctahedral mica and further transformation of the vermiculite into smectite. However, direct formation of illite-smectite at the expense of dioctahedral mica with omission of the vermiculitization stage in soils was also reported (e.g. Righi et al. 1999).

Chlorites in soils generally undergo vermiculitization (e.g. Adams and Kassim 1983; Argast 1991; Bain 1977; Murakami et al. 1996). According to Banfield and Murakami (1998), Churchman and Lowe (2012) and literature cited therein, Proust et al. (1986), Środoń (1999) and Wilson (1999 and literature cited therein, 2004), the vermiculitization of trioctahedral chlorite proceeds via depletion of Fe and Mg and by only a slight loss of Al and leads to the formation of dioctahedral species. Further transformation of chlorite-derived vermiculite into smectite was also reported, for example by Carnicelli et al. (1997).

As far as is evident to the authors of the present paper, all available studies concerning chlorite weathering have focused on trioctahedral species, whereas no study into weathering of dioctahedral species such as di- or tri-sudoite is available. Weathering of micas and chlorites in soils appears not to be understood in detail, clearly indicating a need for detailed mineralogical studies into weathering of the clays in soils.

Some studies indicated that in homogeneous soils developed on acidic parent materials, the transformation of clay minerals is very complex and may be differentiated (e.g. Egli et al. 2001, 2002, 2007; Skiba 2007; Szymański et al. 2017; Uzarowicz and Skiba 2011; Vicente et al. 1977; Waroszewski et al. 2016). According to these studies, it could be supposed that in stratified soils formed on slope deposits rich in sedimentary rocks, transformation of clay minerals would also proceed in various directions. However, in such an environment, usually, an additional element needs to be taken into account: calcium carbonate, which may affect the final modification of clay minerals composition. Soil carbonates (i.e. carbonate minerals such as calcite and dolomite) are regarded as the main constituents known to act as buffering agents, which control soil pH and the rate of soil weathering (Drewnik et al. 2014). Hence, one may expect that the presence of calcium carbonate, both lithogenic and pedogenic, originated from carbonate-rich slope deposits, will influence formation and transformation of clay minerals (Emadi et al. 2008; Khormali and Abtahi 2003; Küfmann 2008). Many authors have described clay mineralogy in carbonate soils (Table 1), yet a comprehensive study concerning a sequence of soils, showing various calcium carbonate distributions and developed on slope sediments of menilite shale, is not available. Therefore, we wanted to test if, in the soils developed on slope deposits with a predominance of menilite shale, and characterized by different content and distributions of calcium carbonate, the clay mineral transformation would reveal multidirectional paths of secondary phase weathering, or if transformation of clay minerals in such stratified materials would reveal only one trajectory.

## 2 Study area and sampling sites

The study was carried out in the Kacwin Village, located in the Western Carpathians in South Poland (Table 2) on the middle and upper part of the slope (Fig. 1). The following geologic series, formed from Upper Cretaceous to Palaeogene, occur at the sampling area: shales and sandstone with beds of conglomerate, shales with Fe-bearing dolomites, and coarse-grained sandstone with conglomerate and shales (Kulka et al. 1985). However, the parent material for the studied profile consisted of menilite shale (Table 2, Fig. 1).

The Western Carpathian soils are not uniformly carbonate-derived; the spatial distribution of soils in the Carpathians is a function of geology, relief, climate and vegetation, resulting in a clear vertical and horizontal soil zonality (Skiba 1995). According to the WRB (IUSS Working Group WRB 2015), within the Western Carpathians, Dystric/Eutric Cambisols, developed from poorly permeable loamy-clayish flysch rocks, are the dominant soil unit. On carbonate-rich parent materials, various types of Leptosols frequently occur. Moreover, on silty-rich parent material within the Carpathian Foothills, Luvisols and Stagnic Luvisols developed. Upper mountain zones are often occupied by Regosols. A small part of the Western

**Table 1** Clay minerals composition in soil developed from calcium carbonate-rich parent material world-wide

| Author(s) | Location | Climate | Parent material | Soil Classification according to Soil Survey Staff (2010, 2014) | Soil Classification according to IUSS, Working Group (2015) | Clay minerals |
|---|---|---|---|---|---|---|
| Kacprzak and Derkowski (2007) | Pieniny Mts. (S Poland) | Temperate | Shale, sandstone, silitstone, limestone | – | Leptosols | Al-mica, illite, illite-smectite mixed-layered minerals, chlorite, chlorite rich mixed-layered minerals, illie-vermicullite, chlorite-vermicullite |
| Costantini and Damiani (2004) | Tuscany (Italy) | Mediterranean | Limestone, dolomite | – | Leptosols, Cambisols, Luvisols | Illie, kaolinite, chlorite, illlite-hiv, illite-chlorite, hiv |
| Rate and Sheikh-Abdullah (2017) | Kurdistan Region (Iraq) | Semi-arid | Limestone, shale, sandstone | Kastanozems Xerolls | – | Smectite, kaolinite, mica, chlorite, vermicullite |
| Zhang et al. (2017) | Beibei Chongqing (China) | Subtropical | Calcarous mudstone | – | Regosols | Kaolinite, smactite, illite, vermicullite, mica |
| Drewnik et al. (2014) | Kraków (S Poland) | Temperate | Jurassic limestone, dolomite covered by loess and gravel | – | Chernozems, Luvisols, Albeluvisols | Mica, biotite, chlorite, kaolinite, smectite, mica-vermicullite, mica-smecitite |
| Oliveira et al. (2018) | Rio Grande de Norte (Brasil) | Semi-arid | Limestone, dolomite | – | Cambisols | Micas group minerals, illite, kaolinite, smectite |
| Khormali and Abtahi (2003) | Fars Province (S Iran) | Arid, semi-arid | Limenstone | Aridosols, Entisols, Alfisols, Mollisols | – | Chlorite, illite, smecticie, palygorskite, kaolinite, chlorite-smectite-vermiculite |
| Pal et al. (2003) | Indo-Gangetic Plains (India) | Semi-arid | Calcarous alluvium | Alfisols | – | Mica, vermiculite, smectite |
| Egli et al. (2008) | Brenta (Italy) | Humid | Limestone, dolomite | – | Cambisol, Leptosol | Mica, vermiculite, chlorite |
| Ferreira et al. (2016) | Apodi Plateau (Brazil) | Semi-arid | Sandstone, limestone, dolomite | – | Cambisols | Smectite, illlite, kaolinite |
| Zagórski (2010) | Małopolska Uplans (S Poland) | Temperate | Devoniam and jurassic limestone | – | Leptosols | Smectite, illite, kaolinite, illite/smectite |
| Ajami et al. (2018) | Nothern Iran | Semi-arid | Calcarous loess | – | Calcisols, Anthrosols, Luvisols | Illie, chlorite, kaolinite, smectite, vermiculite |

–, not determined

**Table 2** Location sites and general information of soil profiles

| Soil profile | Profile No/GPS position/ slope rating/exposure/ elevation a. s. l. | Landform and topography | Stratigraphy | Parent material | Vegetation | WRB classification (WRS, IUSS Working Group 2015) | USDA Soil Taxonomy (Soil Survey Staff 2014) |
|---|---|---|---|---|---|---|---|
| K1 | 49° 22′ 10.7″ N 20° 17′ 11.4″ E 15° NE 551 m a. s. l. | S, UP | Eocene, Oligocene | Menilite shale, red sandstone | HS | Haplic Luvisol (Episiltic, Amphiloamic, Ochric, Ruptic) | Aquic Hapludalf |
| K2 | 49° 22′ 06.7″ N 20° 16′ 51.3″ E 15° NE 650 m a. s. l. | S, MS | Eocene, Oligocene | Menilite shale | HS | Calcaric Eutric Stagnosol (Amphiloamic, Aric, Colluvic, Ruptic, Endoskeletic) | Albaquic Hapludalf |
| K3 | 49° 22′ 01.4″ N 20° 16′ 38.0″ E 5° E 723 m a. s. l. | S, MS | Eocene, Oligocene | Menilite shale, sandstone | FS | Endoskeltic Endocalcaric Luvisol (Anositic, Endoloamic, Colluvic, Ochric, Ruptic) | Aquic Hapludalf |
| K4 | 49° 22′ 06.7″ N 20° 16′ 51.3″ E 5° E 720 m a. s. l. | S, MS | Eocene, Oligocene | Menilite shale | FS | Abruptic Stagnic, Skeletic Luvisol (Ruptic) | Aquic Hapludalf |

Landform and topography: *S*, sloping land; *UP*, upper slope; *MS*, middle slope

Vegetation: *FS*, semi-decidous forest; *HS*, short grassland

Carpathians is covered by Gleysols and Histosols, mostly characterized by considerable fragmentation (Skiba 1995).

Mean annual air temperature for the Western Carpathians ranges between 6 and 8 °C at 700 m.a.s.l., and between 4 and 6 °C at 1100 m.a.s.l. (Otrębska-Starklowa et al. 1995). Mean annual precipitation varies between 400 and 900 mm. The sum of evaporation that can be achieved in the period from May to October is between 300 and 400 mm. The duration of snow cover reaches about 120 days per year on the highest peaks (Otrębska-Starklowa et al. 1995).

The vegetation at the sampling sites is dominated by semi-deciduous forest and short grassland plant habitats characteristic of lower montane zones (Towpasz and Zemanek 1995). The semi-deciduous forest consists of the *Dentario glandulosae-Fagetum* association, where mainly *Fagus sylvatica*, *Abies alba* and *Acer pseudoplantus* occur. Within the lower mountain zone,

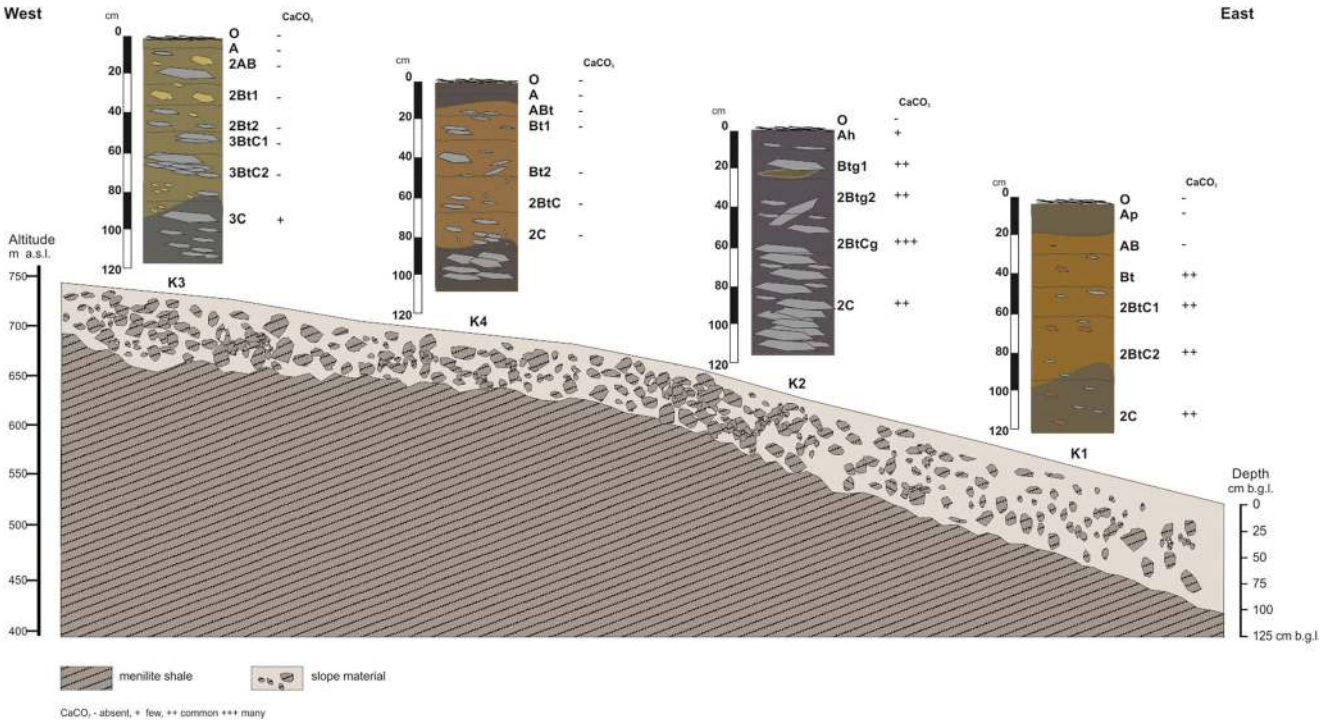


**Fig. 1** Photographs and simplified drawings of studied soil profiles. $CaCO_3$ (g $kg^{-1}$): < 10: +; 10–100: ++; > 100: +++

the *Caltho-Alnetum* association, with *Alnetum incanae* and *Alnus incana*, is relatively common (Towpasz and Zemanek 1995).

## 3 Materials and methods

### 3.1 Field procedures

Soil samples for the present study were collected from four soil pits (24 genetic horizons in total) for further physicochemical, mineralogical, micromorphological and geochemical analyses. The complete raw dataset were made available in public repository Zenodo (Kowalska et al. 2020, https://zenodo.org/record/3972136#.XymDmIgzbIU). Field description of soils was made in accordance with the FAO (2006). The soils were classified according to the World Reference Base for Soil Resources (IUSS Working Group WRB 2015) and Soil Taxonomy (Soil Survey Staff 2014) (Table 2). Furthermore, based on rules for lithic discontinuity (LD) determination given by the WRB (IUSS Working Group 2015), the present LDs have been described in the studied soil profiles.

The chosen soils, located on slopes, were examined in the sequence in which calcium carbonate played different roles: (i) parent material is rich in calcium carbonate, and soil material from every horizon evidently indicated enrichment in calcium carbonate—profile K2; (ii) calcium carbonate occurred in the middle (Bt) and lower (BC or C) part of soil profile—profile K1; (iii) calcium carbonate occurred only within the lowermost horizon (C)—profile K3; (iv) parent material is enriched in calcium carbonate, but the soil mantle does not evidence calcium carbonate enrichment—profile K4 (Fig. 1).

### 3.2 Texture and chemical properties

The soil texture was determined using the Bouyoucos aerometric (Van Reeuwijk 2002). Potentiometric measurements of pH were taken using a standard combination electrode and a CPI-551 Elmetron pH meter in 1 mol $dm^{-3}$ KCl solution and in $H_2O$ at a ratio of 1:2.5 according to the method given by Van Reeuwijk (2002). The content of total organic carbon (TOC) was determined by applying the Tiurin method, using potassium dichromate and Mohr's salt. The content of total nitrogen (Nt) was determined using the Kjeldahl method on a FOSS Kjeltec TM 8100 apparatus. Total $CaCO_3$ content was determined using the Scheibler method with hydrochloric acid (Van Reeuwijk 2002).

### 3.3 Bulk and clay mineralogy (sample preparation and X-ray diffractometry techniques)

Mineral composition was studied for the upper (A horizons), middle (B horizons) and lower (BC/C horizons) parts of sampled soil profiles K1–K4 (K1: Ap, Bt, 2C; K2: Ah, 2Btg2, 2C; K3: A, 2Bt1, 3C; K4: A, Bt2, 2C), and for four samples from the parent material (menilite shale).

To prepare samples for the clay mineral analysis, bulk soil materials (i.e. fractions < 2 mm) and pre-ground (to pass through a 0.4-mm sieve) parent rocks were first treated with acetic acid buffer (pH ~ 5) in order to remove calcium carbonate and divalent exchangeable cations. Organic matter was removed using 15% hydrogen peroxide buffered with an acetic acid buffer. The free Fe-oxides were removed from each sample according to the method of Mehra and Jackson (1960). After the treatment, both bulk clay (< 2 μm) and fine clay (< 0.2 μm) fractions were separated by centrifugation. The clay fractions were split into two portions. One of them was K-saturated and the other was Mg-saturated. Oriented mounts having the surface density of 10 mg $cm^{-2}$ clay were resuspended using an ultrasonic probe in deionized water on petrographic glass slides. Mg-saturated bulk clays were also side-loaded to obtain random powder mounts (Środoń et al. 2001).

X-ray diffraction analyses were registered using a Philips X'Pert diffractometer with vertical goniometer PW3020, equipped with a 1° divergence slit, 0.2 mm receiving slit, incident- and diffracted-beam Soller slits, 1° anti scatter slit, and a graphite diffracted-beam monochromator. Cu-K alpha radiation was used with an applied voltage of 40 kV and 30 mA current. Oriented and random mounts were scanned from 2° to 52° 2θ with a counting speed of 2 s per 0.02° 2θ step (oriented mounts), and from 2° to 65° 2θ with a counting speed of 5 s per 0.02° 2θ step, respectively. The analyses of the oriented slides were performed in air-dried conditions, after liquid glycerol solvation (for Mg-saturated samples) and after 1 h heating at 330 °C and 550 °C sequentially (for K-saturated samples). The XRD patterns were processed using the ClayLab computer program (Mystkowski 1999).

Fourier-transform attenuated total reflectance infrared (FTIR-ATR) spectra were collected for Mg-saturated < 2 μm fractions separated from each of the studied samples. A total of 32 scans were collected for each spectrum in the range from 400 to 4000 $cm^{-1}$ with a resolution of 2 $cm^{-1}$ with a Thermo Nicolette Is50 spectrometer equipped with a Pike Technologies MIRacle™ single reflection horizontal ATR accessory. The spectra were processed using the OMNIC computer program.

### 3.4 Operational definitions used during the identification of clay minerals

Mica (illite) was identified by the presence of peaks at 1.0, 0.33, 0.50, 0.25 and 0.20 nm, which did not change the positions and the intensities after any diagnostic treatments (Moore and Reynolds 1997). Peaks at 0.72 nm and 0.358 nm were attributed to kaolinite (Brown and Brindley 1984; Moore and Reynolds 1997; Środoń 2006), and they disappeared after heating to 550 °C.

Vermiculite was identified in the air-dried Mg-exchanged form the basal reflection near 1.40 nm. The reflection did not change its position after solvation with liquid glycerol. However, it moved to ~ 1.0 nm after heating at 330 °C for 1 h (Moore and Reynolds 1997; Środoń 2006).

Chlorite was identified by the reflection near 1.4 nm, present in XRD patterns registered for Mg-saturated samples at air-dry conditions and after liquid glycerol solvation. The reflection did not change its position after heating at 330 °C and moved to 1.27 nm after heating at 550 °C. This behaviour allowed chlorite to be distinguished from vermiculite (Moore and Reynolds 1997; Środoń 2006). Mixed-layered clay minerals were identified based on the Méring principle (Méring 1949).

### 3.5 Geochemistry

The 0.1 g of each sample has been mixed with 1.0 g of $Li_2B_40_7$ flux. Such prepared mixture have been put into the crucibles. Further, the crucibles have been transferred to a furnace that was previously heated to 1100 °C. During at least 30 min, the samples were fused to ensure good homogeneity. After the fusion, the crucibles have been left to cool. The fused sample has been taken out and moved into a beaker that containing about 40 ml deionized water and 4 ml of nitric acid in order to dissolve. After the full dissolution, the obtained solution has been transferred to the flasks using deionized water (Delijska et al. 1988; Yu et al. 2003). Such prepared samples were analysed using inductively coupled plasma optical emission spectroscopy (ICP-ES) with a Spectro Ciros Vision and inductively coupled plasma mass spectrometry (ICP-MS) with a PerkinElmer ELAN 9000 in Acme Labs, Bureau Veritas (Canada). The detection limit for $SiO_2$, $Al_2O_3$, MgO, CaO, $Na_2O$ and $K_2O$ was 0.01% and 0.04% for $Fe_2O_3$. Whereas, detection limit of Hf and Zr was 0.01 ppm.

In order to assess the potential influence of weathering on clay mineral composition, two indices of weathering have been calculated: Chemical index of alternation (CIA) (1) and compositional variability (ICV) (2) (Cox et al. 1995; Fiantis et al. 2010; Goldberg and Humayun 2010; Nesbitt and Young 1982; Pasquini et al. 2017).

$$\mathrm{CIA} = 100 \times \frac{Al_2O_3}{Al_2O_3 + CaO + Na_2O + K_2O} \quad (1)$$

The CIA quantitatively represents the degree of primary feldspar transformation into secondary clay minerals. The typical fresh value for CIA is ≤ 50, and the typical weathered value is 100 (Depetris et al. 2014; Fiantis et al. 2010; Pasquini et al. 2017).

$$\mathrm{ICV} = \frac{(Fe_2O_3 + \mathrm{K_2}O + Na_2O + CaO + MgO + SiO_2)}{Al_2O_3} \quad (2)$$

The ICV measures the abundance of alumina relative to other major constituents of the rock, except $SiO_2$. The values of ICV higher than 1.2 suggest that the soil material is immature, while values lower than 1.0 indicate maturity of soil (Depetris et al. 2014; Pasquini et al. 2017).

### 3.6 Preparation and description of soil and rock thin sections

Sampled soils and menilite shale (parent material) fragments were embedded in a polyester Polimal® 108 resin using an Epovac vacuum chamber (Struers®). Thin sections were prepared using a CS30 saw for soil sample cutting (Struers®), a CL50 apparatus for precision lapping of thin sections (Logitech®) and a CL50 apparatus for thin section polishing (Logitech®). Mineralogical description of polished thin sections was carried out using a Nikon Eclipse 400 microscope. Each thin section description was elaborated in accordance with the nomenclature proposed by Stoops (2003).

## 4 Results

### 4.1 Field characteristics and soil texture

The studied soils were classified as Luvisols (K1, K3 and K4) and a Stagnosol (K2) with various principal and supplementary qualifiers according to WRB rules (Table 2). Considering the assumptions given by Soil Taxonomy (Soil Survey Staff 2014), the soils were classified as Aquic Hapludalfs (K1, K3 and K4) and Albaquic Hapludalf (K2) (Table 2). The soils represented various degrees of stratification. At least one lithic discontinuity (LD) was recognized per soil profile based on grain size distribution and changes in coarse fragment content; hence, ruptic qualifier was applied within each soil profile (Fig. 2, Table 3 and Table S1). The soil K1, located in the lowest part of the slope, showed high homogeneity in terms of coarse fragment content: about 5% of angular shaped coarse fragments occurred in each soil horizon (Table 2). The silt fraction prevailed, giving rise to the silty loam texture to a depth of 50 cm, where LD was recognized. In the lower horizons, silty clay loam texture was recognized (Fig. 2; Table S1). In the soil K2, located in the middle slope section, the content of coarse fragment suddenly increased at a depth of 25 cm, pointed to LD presence and reached the value of 80% in horizon 2C (Table 3). Similarly, the silt fraction predominated in this soil; the loam (horizon A) and silt loam textures (horizons Btg1, 2Btg2, 2BtCg, 2C) were recognized (Fig. 2, Table S1) which also suggested heterogeneity in terms of grain size distribution. The increase in coarse fragment towards the bottom of the profile was seen also in soil K3; however, in this soil, the A horizon indicated very low content

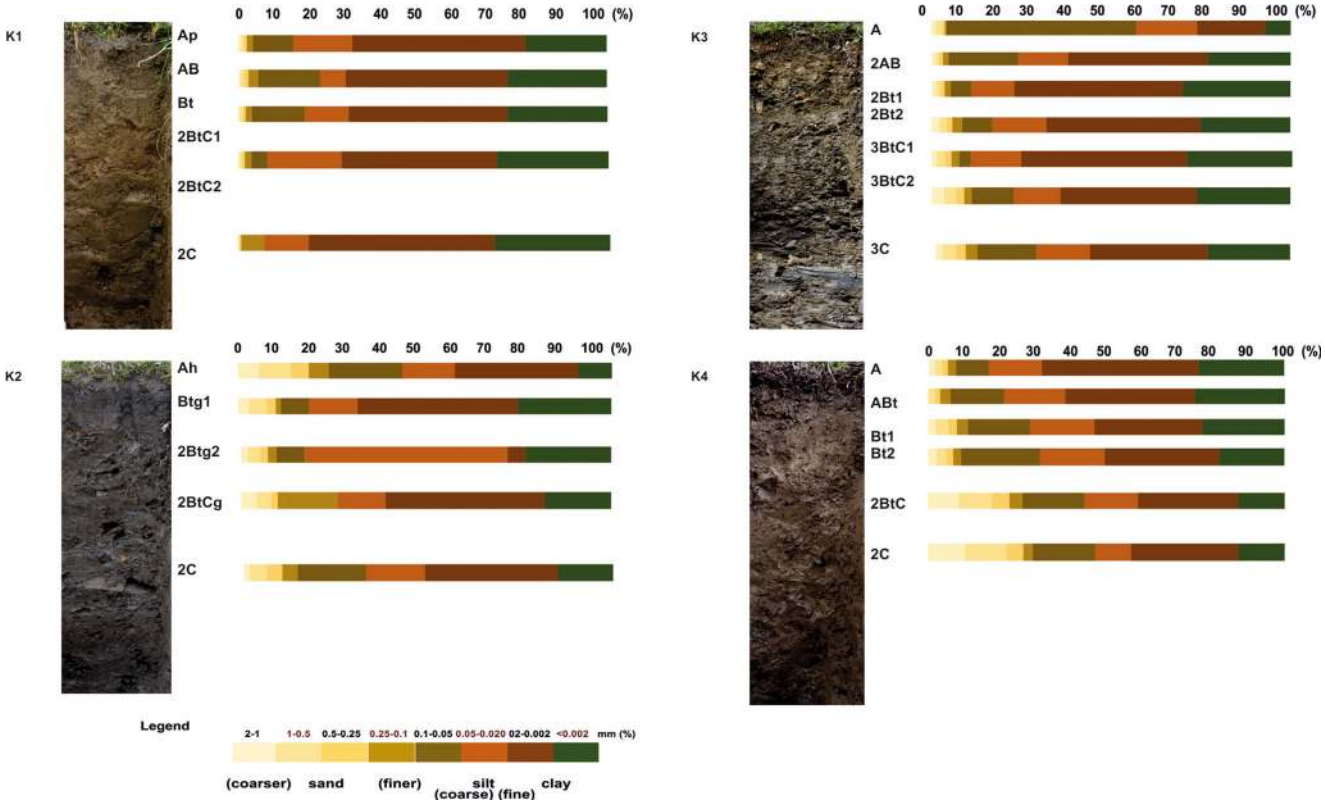


**Fig. 2** Depth plots of grain size distribution within soil profiles

of coarse fragment (5%) (Table 3). The soil K3 was characterized by the highest content of silt compared to the other profiles. However, very high heterogeneity was recognized in terms of texture group in this profile (Fig. 2, Table S1). The A horizon revealed the sandy loam texture. Below this, the first LD was distinguished through the changes in texture towards the silt loam and silt clay loam. Lower, at a depth of 46 cm, another LD was recognized based on the increase in coarse fragments as well as changes in grain size distribution towards more clayish texture. The soil K4 was characterized by the high content of coarse fragment (40–90%, Table 3), which increasing with the depth. The A and ABt horizons represented the silt loam texture; below this, loam texture was recognized (Fig. 2, Table S1). At a depth of 51 cm, the LD was recognized and manifested itself by change in grain size distribution as well as a sudden increase in coarse fragments.

## 4.2 Chemical properties

The studied profiles represented different patterns of primary $CaCO_3$ distribution. Profile K1 was characterized by the presence of $CaCO_3$ in the Bt, 2BtC1, 2BtC2 and the 2C horizons. The content of $CaCO_3$ ranged from 12.6 to 17.0 g $kg^{-1}$. The $CaCO_3$ within profile K2 occurred in every horizon, and its content ranged from 1.60 to 92.1 g $kg^{-1}$, gradually increasing downward through the soil profile. Within profile K3, the $CaCO_3$ content was present only in the 3C horizon (9.87 g $kg^{-1}$). No $CaCO_3$ was noted in profile K4 (Table 4). Soils K3 and K4 indicated the lowest pH values, in some horizons pointing towards a slight acidic reaction, whereas the soil horizons of K1 and K2 were characterized by neutral and alkaline reactions. The content of TOC and Nt ranged from 3.1 to 133 g $kg^{-1}$ and from 0.83 to 8.1 g $kg^{-1}$ respectively (Table 4).

## 4.3 Clay mineralogy

### 4.3.1 Clay minerals composition of the studied soil horizons and parent material

Clay fractions separated from all studied soils showed very similar XRD patters. In all fine clays (fractions < 0.2 μm), illite, vermiculite and kaolinite were identified (Fig. 3 ((a, b)). Superstructure reflections and the higher order reflections observed in XRD patterns of Mg-saturated samples at ~ 2.4 nm and 1.2 nm, and at ~ 2.8 nm and ~ 1.4 nm, registered at air-dry conditions and after glycerol solvation (Fig. 3 ((a)) respectively, indicated a presence of partly ordered illite-smectite mixed-layered minerals (i.e. R1 I-S). Bulk clays (i.e. fractions < 2 μm), except illite, vermiculite and R1 I-S, also contained traces of chlorite (Fig. 4). Weak reflections at ~ 0.8 nm, observed in XRD patterns of K-saturated bulk clays registered after heating at 330 °C, most likely indicated a

**Table 3** Morphological characteristics of the studied soils

| Soil profile | Depth (cm) | Soil horizon | Boundary | Munsell colour* | Coarse fragments | Shape of coarse fragments | Abundance of clay coatings ** | Calcium carbonate ** | Structure | Consistence | Moisture | Abundance of roots | Texture*** |
|---|---|---|---|---|---|---|---|---|---|---|---|---|---|
| K1 | 3–0 | O | A,S | n.d. | n.d. | n.d. | – | – | n.d. | n.d. | n.d. | n.d. | n.d. |
| | 0–20 | Ap | A, S | 10YR 4/6 | n.d. | n.d. | + | – | ME MO CR | FR | SM | F | SiL |
| | 20–33 | AB | G, S | 10YR 4/4 | 5 | A | + | – | ME ST SB | FR | M | N | SiL |
| | 33–50 | Bt | G, S | 10YR 5/4 | 5 | A | ++ | ++ | ME ST SB | FI | M | N | SiL |
| | 50–70 | 2BtC1 | G, S | 10YR 5/4 | 5 | A | +++ | ++ | ME ST AB | FI | M | N | SiCL |
| | 70–110 | 2BtC2 | G, S | 10YR 5/4 | 5 | A | +++ | ++ | ME ST AB | VFI | M | N | SICL |
| | >110 | 2C | – | 10YR 4/4 | 5 | A | ++ | ++ | ME ST AB | VFI | M | N | SiCL |
| K2 | 2–0 | O | G,W | n.d. | n.d. | n.d. | – | – | n.d. | n.d. | n.d. | n.d. | n.d. |
| | 0–9 | Ah | G, W | 10YR 42 | 10 | A | ++ | + | ME MO CR | FI | SM | M | L |
| | 9–25 | Btg1 | G, S | 2.5Y 4/6 | 30 | A | +++ | ++ | ME MO AB | FI | SM | F | SiL |
| | 25–52 | 2Btg2 | G, S | 2.5Y 4/4 | 70 | A | +++ | ++ | ME MO AB | FI | M | VF | SiL |
| | 52–76 | 2BtCg | G, S | 2.5Y 3/3 | 70 | A | ++ | +++ | ME MO SB | VFI | M | N | SiL |
| | 76–105 | 2C | – | 2.5Y 3/3 | 80 | A | ++ | ++ | ME MO AB | VFI | M | N | SiL |
| K3 | 2–0 | O | G, S | n.d. | n.d. | n.d. | – | – | n.d. | n.d. | n.d. | n.d. | n.d. |
| | 0–8 | A | G, S | 2.5Y 4/4 | 5 | A | + | – | ME MO CR | FR | SM | C | SL |
| | 8–21 | 2AB | G, S | 2.5Y 5/4 | 60 | A | + | – | ME MO AB | FI | SM | C | SiL |
| | 21–31 | 2Bt1 | G, S | 2.5Y 4/2 | 60 | A | +++ | – | CO MO AB | FI | SM | F | SiL |
| | 31–46 | 2Bt2 | G, S | 2.5Y 3/3 | 80 | A | ++ | – | CO MO AB | FI | SM | F | SiL |
| | 46–58 | 3BtC1 | G, S | 2.5Y 3/3 | 70 | A | ++ | – | CO ST AB | VFI | SM | N | SiCL |
| | 58–80 | 3BtC2 | G, S | 2.5Y 3/2 | 90 | A | + | – | CO MO AB | VFI | SM | N | CL |
| | 80–113 | 3C | – | n.d. | 90 | A | +++ | ++ | n.d. | VFI | SM | N | L |
| K4 | 2–0 | O | G,S | n.d. | n.d. | n.d. | – | – | n.d. | n.d. | n.d. | n.d. | n.d. |
| | 0–7 | A | G, S | 10YR 4/2 | n.d. | n.d. | – | – | VF WE CR | FR | D | C | SiL |
| | 7–17 | ABt | G, S | 10YR 4/4 | 40 | A | + | – | CO MO SB | FI | SM | C | SiL |
| | 17–36 | Bt1 | G, S | 10YR 5/4 | 60 | A | + | – | CO MO SB | FI | SM | F | L |
| | 36–51 | Bt2 | G, S | 10YR 5/3 | 60 | A | ++ | – | CO MO SB | FI | SM | N | L |
| | 51–70 | 2BtC | G, S | 10YR 5/6 | 80 | A | + | – | CO MO SB | VFI | SM | N | L |
| | 70–90 | 2C | – | 10YR 5/4 | 90 | A | + | – | CO MO SB | VFI | SM | N | L |

* according to Munsell Colour Charts (1975); ** clay coatings and $CaCO_3$ quantity: – absent, + few, ++ common +++ many; *** texture (FAO, 2006): *SL*, sandy loam; *SiL*, silt loam; *SiCL*, silty clay loam; *CL*, clay loam; *L*, loam; *C*, clay

Boundary (FAO, 2006): Distinctness: *A*, abrupt; *G*, gradual, Topography: *S*, smooth; *W*, wavy

Shape of coarse fragments: *A*, angular

Structure (FAO, 2006): (1) Size classes: *VF*, very fine; *FI*, fine, *ME*, medium, *CO*, coarse, *CV*, very coarse. (2) Types of structure: *CR*, crumby; *AB*, angular blocky; *SB*, subangular blocky. (3) Classification of structure: *WE*, weak; *MO*, moderate; *ST*, strong

Consistence (FAO, 2006): *FR*, friable; *FI*, firm, *VFI*, very firm

Moisture (FAO, 2006): *SM*, slightly moist; *M*, moist

Abundance of roots (FAO, 2006): *N*, none; *V*, very few; *F*, few; *C*, common; *M*, many

*n.d.*, not determined

**Table 4** Chemical properties of the studied soils

| Soil profile | Depth (cm) | Soil horizon | pH | | $CaCO_3$ | TOC | Nt | C:N |
|---|---|---|---|---|---|---|---|---|
| | | | $H_2O$ | KCl | g $kg^{-1}$ | | | |
| K1 | 3–0 | O | n.d. | n.d. | n.d. | n.d. | n.d. | n.d. |
| | 0–20 | Ap | 5.9 | 4.4 | n.d. | 28.0 | 3.46 | 8.09 |
| | 20–33 | AB | 6.6 | 4.3 | n.d. | 10.6 | 1.48 | 7.18 |
| | 33–50 | Bt | 6.4 | 4.2 | 17.0 | 5.00 | 1.22 | 4.11 |
| | 50–70 | 2BtC1 | 6.2 | 3.9 | 14.3 | 4.20 | 1.23 | 3.42 |
| | 70–110 | 2BtC2 | 6.2 | 3.8 | 12.6 | 3.10 | 0.83 | 3.72 |
| | > 110 | 2C | 6.2 | 3.8 | 16.7 | 4.20 | 1.15 | 3.64 |
| K2 | 2–0 | O | n.d. | n.d. | n.d. | n.d. | n.d. | n.d. |
| | 0–9 | Ah | 6.7 | 6.4 | 1.60 | 40.0 | 4.41 | 9.07 |
| | 9–25 | Btg1 | 8.0 | 7.7 | 27.3 | 8.21 | 1.23 | 6.67 |
| | 25–52 | 2Btg2 | 8.0 | 7.9 | 57.1 | 6.95 | 1.02 | 6.81 |
| | 52–76 | 2BtCg | 8.3 | 7.8 | 92.1 | 4.98 | n.d. | n.d. |
| | 76–105 | 2C | 8.4 | 7.9 | 92.1 | 5.17 | n.d. | n.d. |
| K3 | 2–0 | O | n.d. | n.d. | n.d. | n.d. | n.d. | n.d. |
| | 0–8 | A | 5.3 | 3.3 | n.d. | 25.0 | 2.40 | 10.4 |
| | 8–21 | 2AB | 5.4 | 3.8 | n.d. | 10.9 | 2.60 | 4.30 |
| | 21–31 | 2Bt1 | 5.8 | 4.1 | n.d. | 8.80 | 2.30 | 3.80 |
| | 31–46 | 2Bt2 | 6.1 | 4.7 | n.d. | 29.0 | 0.90 | 30.7 |
| | 46–58 | 3BtC1 | 5.9 | 4.7 | n.d. | 31.7 | 2.50 | 12.6 |
| | 58–80 | 3BtC2 | 5.8 | 4.8 | n.d. | 36.8 | 1.00 | 38.7 |
| | 80–113 | 3C | 6.7 | 5.9 | 9.87 | 39.6 | 3.00 | 13.3 |
| K4 | 2–0 | O | n.d. | n.d. | n.d. | n.d. | n.d. | n.d. |
| | 0–7 | A | 5.6 | 3.6 | n.d. | 133 | 5.60 | 23.8 |
| | 7–17 | ABt | 6.6 | 4.7 | n.d. | 35.3 | 8.10 | 4.40 |
| | 17–36 | Bt1 | 5.4 | 3.3 | n.d. | 34.3 | 4.10 | 8.40 |
| | 36–51 | Bt2 | 5.8 | 3.8 | n.d. | 34.4 | 2.20 | 15.5 |
| | 51–70 | 2BtC | 5.5 | 3.8 | n.d. | 31.1 | 2.50 | 12.7 |
| | 70–90 | 2C | 6.1 | 4.2 | n.d. | 29.6 | 4.10 | 7.30 |

*n.d.*, not determined

presence of ordered vermiculite-chlorite mixed-layered minerals (i.e. R1 V-Ch, Fig. 5).

Unlike clays separated from soil horizons, clay fractions from the parent material samples showed some diversity. Both fine and bulk clays from the parent material of the K1 profile contained chlorite, highly illitic I-S, vermiculite and only traces of kaolinite (Fig. 3 ((a, b)).

Clays (both bulk and fine) separated from parent material of the K2 and K3 profiles showed XRD patterns very similar to clays from the soils and contained illite, R1 I-S, vermiculite, traces of kaolinite and traces of chlorite and R1 V-Ch, the latter two present in bulk clays (Fig. 4). Illite, R1 I-S, vermiculite and traces of kaolinite and chlorite were identified in fine and bulk clays separated from the parent material of the K4 profile (Fig. 3 ((a, b)).

All studied clays seemed to be dioctahedral, as indicated by the positions of the 060 reflections at ~ 0.151 nm in XRD patterns registered for random powder mounts (Fig. 6).

Despite the fact that most of the studied clays gave very similar XRD patterns, some general trends of clay minerals distribution within the profiles could be observed, namely a decrease in the amount of chlorite relative to other phases observed towards the top of profile (best seen in soil K1), and an increase in the amount of R1 I-S relative to illite and vermiculite observed towards the top of the profiles (Fig. 7).

#### 4.3.2 FTIR-ATR measurements

FTIR-ATR spectra (Fig. 8 ((a, b)) of all the soil clays were very similar and showed absorption bands characteristic of aluminous (dioctahedral) 2:1 clays at ~ 3620 $cm^{-1}$ (due to stretching AlOHAl vibrations), ~ 912 $cm^{-1}$ (due to bending AlOHAl vibrations) and ~ 750 $cm^{-1}$ (due to Al-O-Si vibrations) (Russell and Fraser 1994). Absorption bands at 3700 $cm^{-1}$ indicated the presence of kaolinite, whereas bands at ~ 790 $cm^{-1}$ and 780 $cm^{-1}$ indicated small admixtures of

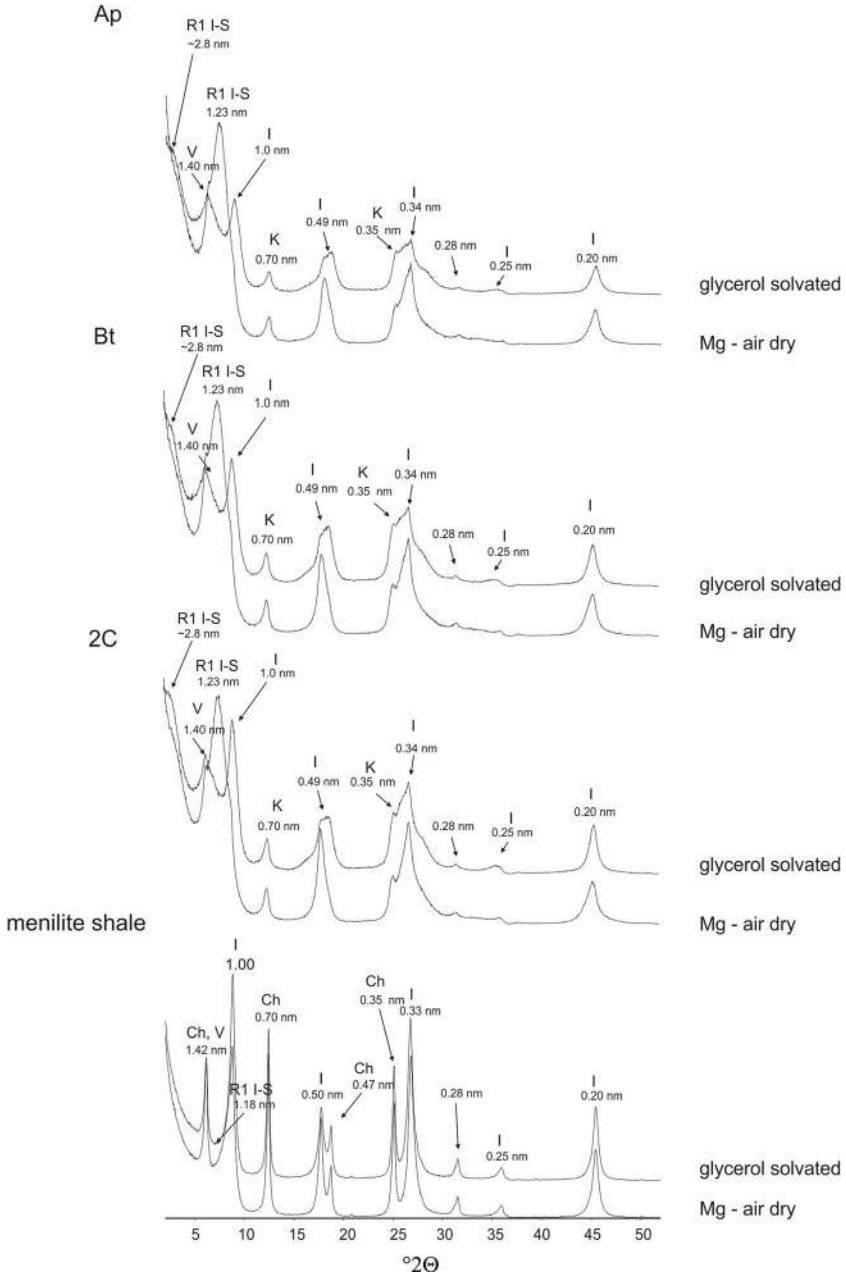


**Fig. 3** (a) XRD patterns of Mg-saturated fine clays (< 0.2 μm fractions) from soil horizons and parent menilite shale of profile (K1) registered at air-dried conditions and after saturation with glycerol. I illite, K kaolinite, V vermiculite, Ch chlorite, R1 I-S R1 illite-smectite, (b) XRD patterns of K-saturated fine clays (< 0.2 μm fractions) from soil horizons and parent menilite shale of profile (K1) registered after heating at 330 °C. I illite, K kaolinite, Ch chlorite, R1 I-S R1 illite-smectite

quartz. A weak band at 827 $cm^{-1}$, assigned to bending AlOHMg vibrations, indicated some Mg for Al substitutions in the octahedral sheets of studied clays (Russell and Fraser 1994). A broad band due to Si-O vibrations typical for all silicates was observed at ~ 1000 $cm^{-1}$. Weak bands at ~ 3300 $cm^{-1}$ and ~ 1430 $cm^{-1}$ may indicate a small amount of $NH_4^+$ fixed within 2:1 phyllosilicate interlayers (Ahlrichs et al. 1972; Stone and Wild 1978; Šucha and Širáňová 1991; Skiba et al. 2018), but the band might also be due to soil organic matter (Russell and Fraser 1994; Skiba et al. 2011). Bands at ~ 1650 $cm^{-1}$ and 3400 $cm^{-1}$ were likely due to adsorbed water (Fig. 8 ((a)).

FTIR-ATR spectra of parent material showed essentially the same pictures as the soil clays, except for spectra collected for parent material of the K1 and K4 profiles (Fig. 8 ((b)). In both these spectra, in the OH-stretching region, additional absorption bands at ~ 3550 $cm^{-1}$ were observed. Those bands indicated the trioctahedral character of interlayer octahedral sheet in aluminous chlorite and, together with a band at ~ 3620 $cm^{-1}$, were indicative of di-trioctahedral chlorite

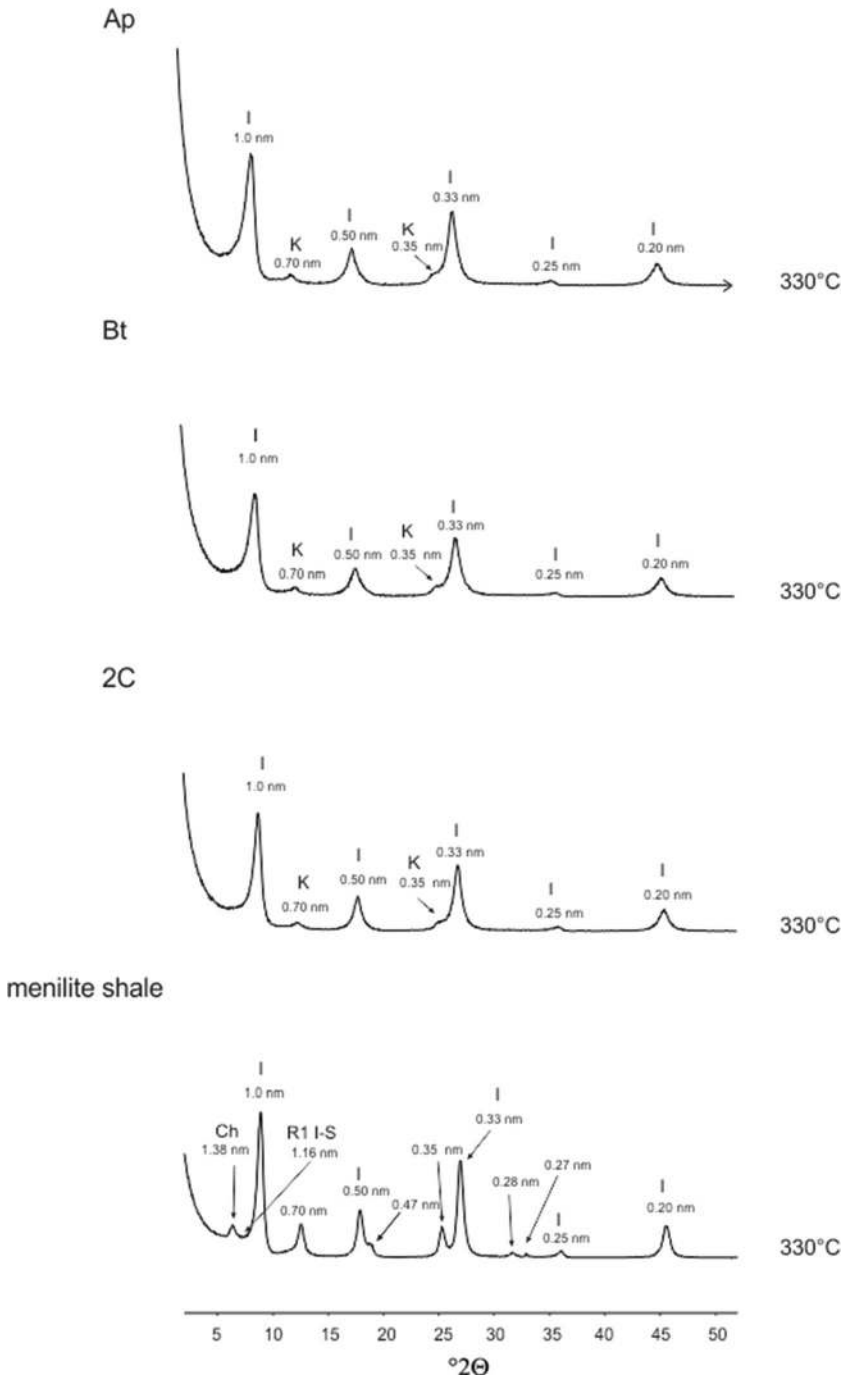


**Fig. 3** (continued)

(sudoite) (Russell and Fraser 1994). In the spectrum of parent material of the K1 profile, no bands indicative of kaolinite were observed at ~ 3700 and at 695 $cm^{-1}$.

### 4.4 Geochemistry

All of the soil horizons were characterized by relatively high content of $SiO_2$ and $Al_2O_3$ (from 50.4 to 61.7% and from 16.0 to 19.6% respectively, Table 5). Additionally, the percentage content of $Fe_2O_3$ exhibited high values (from 6.16 to 8.12%) and demonstrated a more homogeneous arrangement of this oxide within the soil profiles. The content of CaO, which is connected with the distribution of $CaCO_3$, was varied in these profiles (Table 5). The content and distribution of the other major oxides ($K_2O$, MgO and $Na_2O$) was rather homogeneous (Table 5). Further, the low content of stable trace elements like Zr (from 138 to 170 ppm) and Hf (from 3.90 to 5.60 ppm) was noted.

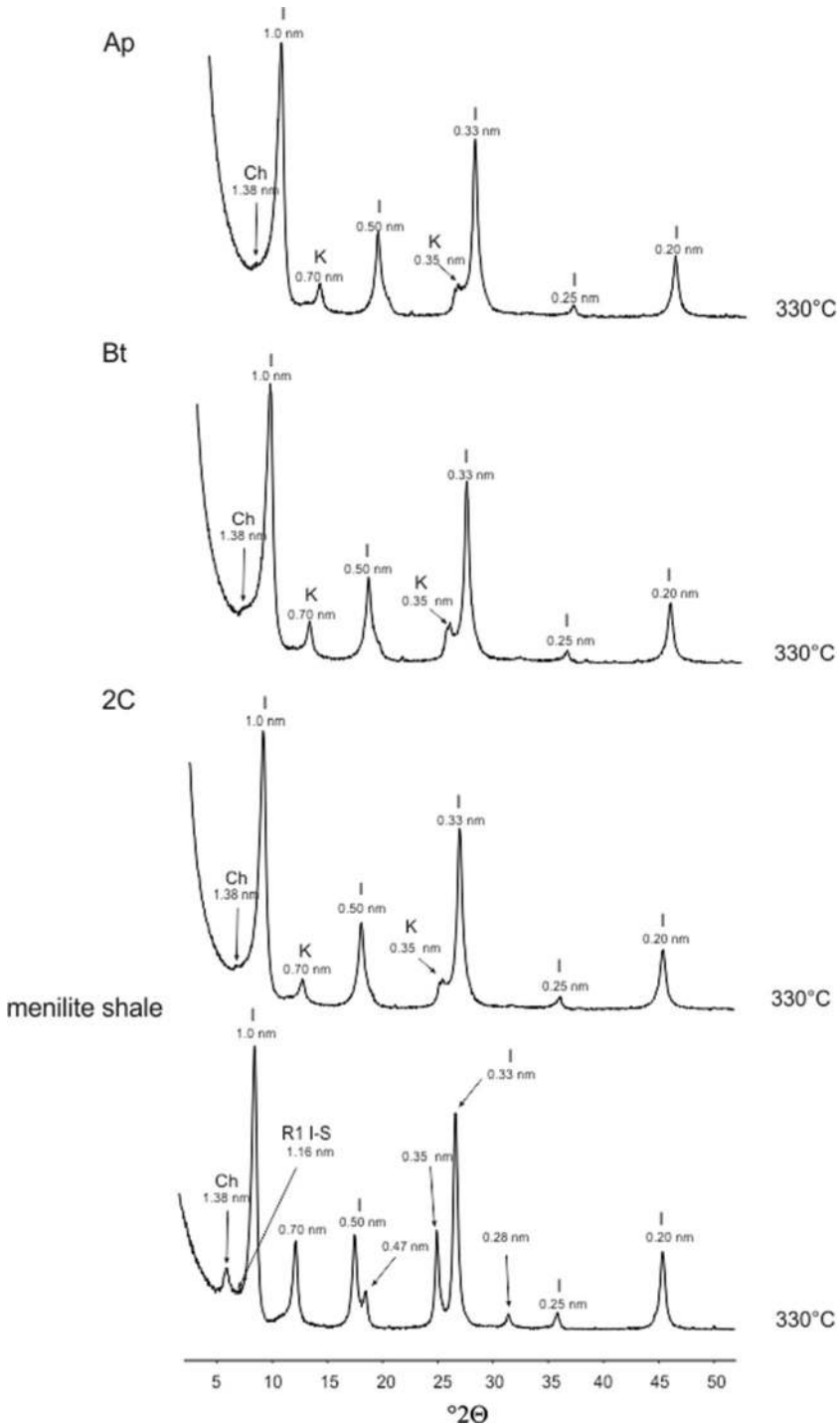


**Fig. 4** XRD patterns of K-saturated bulk clays (< 2 μm fractions) from soil horizons and parent menilite shale of profile (K1) registered after heating at 330 °C. I illite, K kaolinite, Ch chlorite, R1 I-S R1 illite-smectite

To prove the effect of weathering on clay mineral formation, two indices of weathering were calculated (Table 5). The CIA ranged between 59.3 and 80.8, indicating an advanced degree of the weathering process (Pasquini et al. 2017). The ICV values, which ranged between 0.78 and 1.25 (Table 5), suggest that the studied soils are mature. Calculated CIA and ICV did not show large differences between soil horizons, which suggests a similar degree of weathering.

## 4.5 Optical microscopy observations

### 4.5.1 Parent material mineralogy

The menilite shale rock fragments sampled from the studied soils showed a high degree of similarity in terms of mineralogy. Generally, quartz and plagioclase occurred as major components, and a large fraction of micas was noted (Fig. 9).

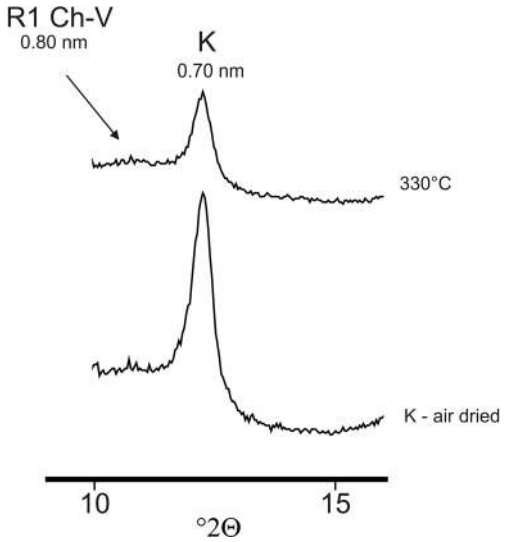


**Fig. 5** XRD patterns of K-saturated bulk clays (< 2 μm fractions) from soil horizon of profile (K1) registered after heating at 330 °C. R1 Ch-V R1 chlorite-vermiculite

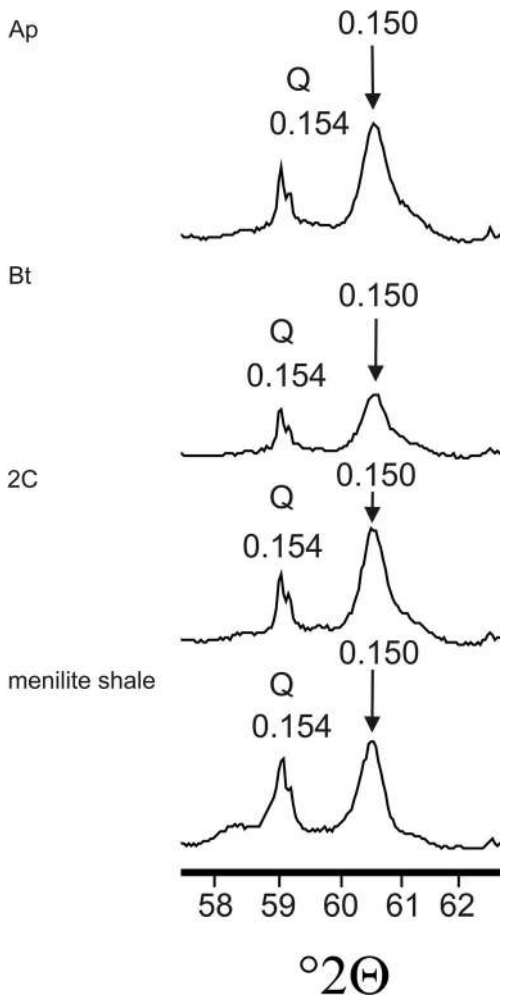


**Fig. 6** 060 region of XRD patterns registered for randomly oriented powder mounts of Mg air-dried bulk clays (< 2 μm fractions) from K1 profile

Further, the clay minerals were identified in each sample (Fig. 9). Locally, carbonate minerals were found, which simultaneously conditioned the carbonate character of the menilite shale. Primary calcium carbonate occurred also in the form of calcite veins within rock fragments (Fig. 9), which was especially visible in the thin sections from K1 and K2. In addition, single glauconite grains were noted (Fig. 9).

#### 4.5.2 Soil micromorphological features

Thin sections from the soil samples were very similar in terms of soil micromorphology features. Soils were characterized mostly by subangular blocky and vughy microstructure (Table S2) and vughs (Fig. 10 (a): IIIa, Va) and planar type of voids (Fig. 10 (a): IIa, Iva, Va; Fig. 10 (b): IIIa, Va). The single space porphyric and double space porphyric c:f–related distribution pattern predominated (Table S2). The soil horizons represented mainly speckled (Fig. 10 (a): IIb, IIIb, IVb), granostriated (Fig. 10 (a): IIIb; Fig. 10 (b); Ib, Vb) and porostriated (Fig. 10 (a): IIb, Vb; Fig. 10 (b): Ib, Vb) types of b-fabric.

The majority of the upper and middle soil horizons were characterized by the occurrence of organ and tissue residues as well as amorphous organic fine material (Table S2). The mineralogical composition in the studied soil was very uniform. Mainly, quartz, feldspar and clay minerals occurred in the studied soil horizons (Table S2). Rock fragments represented menilite shales (Fig. 10 (a): IIIb, IVb, Vb; Fig. 10 (b): Ib, Vb).

The occurrence of pedofeatures was mainly connected with the clay illuviation process. Pedofeatures took the form of crescent clay coatings (Fig. 10 (a): Ib, IIb, IVb; Fig. 10 (b): Vb) and clay infillings (Fig. 10 (a): IIIb, Vb; Fig. 10 (b): Ib, IIb, IIIb) and were seen in almost every horizon of studied soil. Moreover, iron-manganese nodules (Fig. 10 (a): IIb, IIIb; Fig. 9(b): IVb) and iron-manganese impregnations were visible (Fig. 10 (b): IIb, IIIb, IVb).

## 5 Discussion

### 5.1 The origin of identified clay minerals in studied soils

The studied soils contained a wide variety of phyllosilicates (see Section 4.3). The fact that parent material (i.e. menilite shales) of the studied soils contained illite suggested inheritance from the parent material. Inheritance of illite in soils is a well-known phenomenon and has been described by many authors (e.g. Wilson 1999 and literature cited therein). It may be argued that illite is also likely to be formed in soils, and a mechanism of illite formation may involve potassium fixation by dioctahedral high-charge swelling clays, as shown, for example, by Środon and Eberl (1980), and more recently

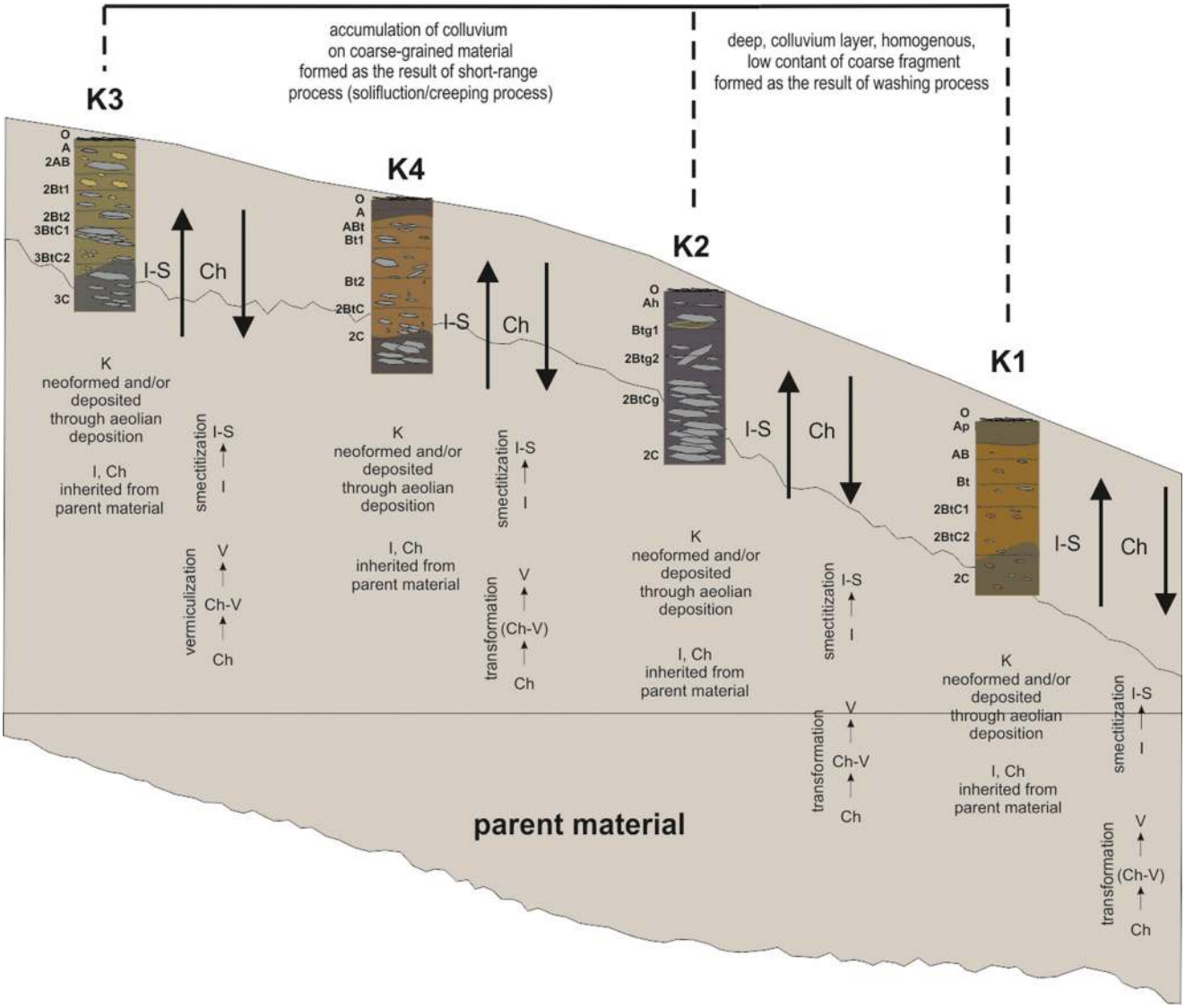


**Fig. 7** Origin of clay minerals and trends among the slope position. Ch chlorite, I-S mixed phase illite-smectite, V vermikulite, I illite, Ch-V mixed phase chlorite-vermiculite, K kaolinite. The clay minerals composition were uniform in each profile; however, two main trends were observed: (i) a decrease in the amount of chlorite relative to other phases observed towards the top of profile, (ii) increase in the amount of R1 I-S relative to illite and vermiculite observed towards the top of profile. Graphic arrangement of the Fig. 7 inspired by Waroszewski et al. (2016)

by Skiba (2013) and Skiba et al. (2018). However, in the studied soils, rather an opposite pathway could be observed—that is, illite transformation towards smectite. The transformation was indicated by the fact that an increase in R1 I-S content relative to illite was observed upwards through the soil profile (Fig. 7). This trend strongly suggested that neoformation of illite in studied soils was unlikely.

Similar to the illite, di-trioctahedral chlorite (sudoite) present in studied soils was most likely inherited from the parent material (i.e. it was of lithogenic origin). This was indicated by the fact that chlorite was abundant in both fine and bulk clays separated from fresh (i.e. unweathered) parent menilite shales from K1 and K4, while fine clays separated from soil materials did not contain chlorite, and the bulk clays contained only traces of chlorite and chlorite-vermiculite mixed-layered minerals (Figs. 3 ((b), 4, and 5). Additionally, chlorite content decreased upward through the soil profiles (Fig. 7) indicating likely transformation and/or dissolution of the mineral in the studied soils.

Dioctahedral vermiculite in the studied soils seems to be a product of chlorite transformation. This is indicated by the fact that the soils, except for discrete dioctahedral vermiculite, contained traces of R1 chlorite-vermiculite mixed-layered minerals. Of course, it could be argued that dioctahedral vermiculite may have been formed at the expense of dioctahedral mica (illite), which is abundant in the parent material. Vermiculitization of dioctahedral mica is a commonly occurring transformation reaction taking place in soils leading to

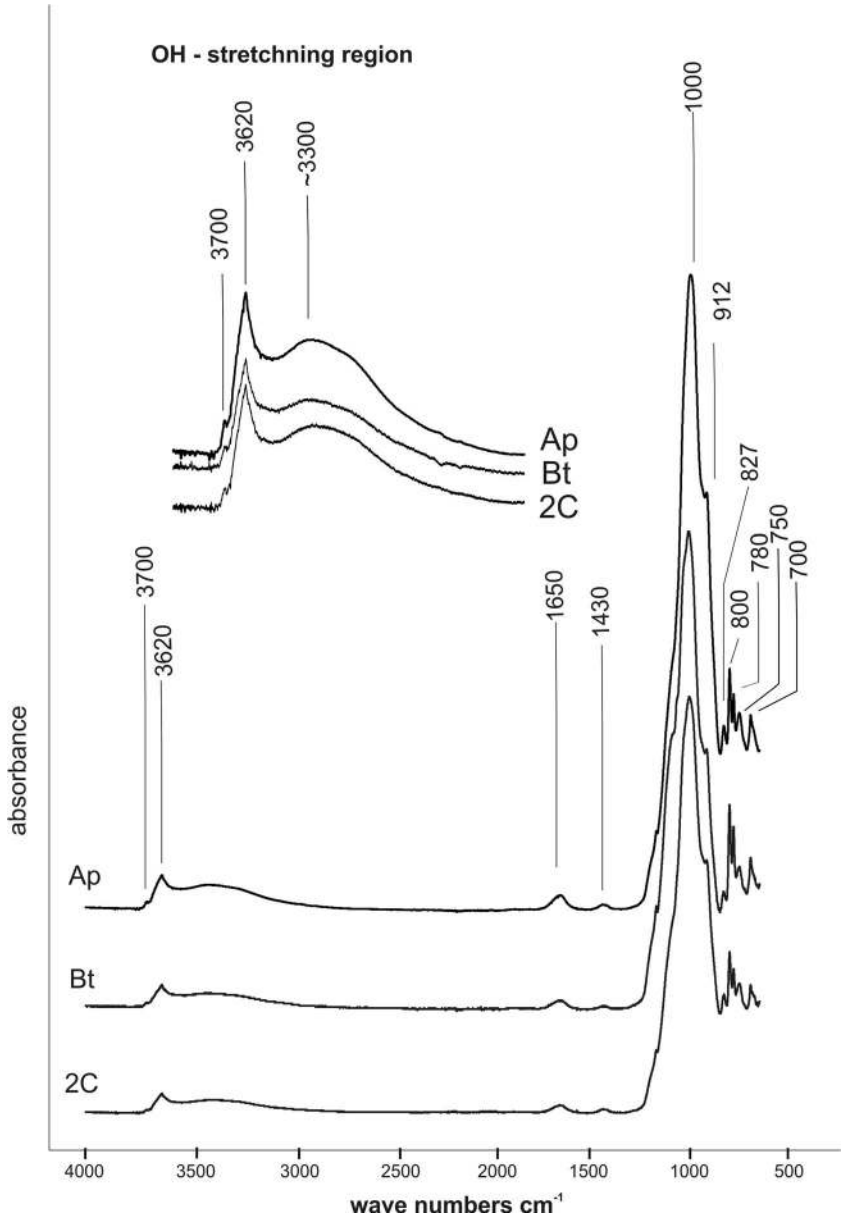


**Fig. 8** (a) FTIR-ATR measurements of selected soil horizons samples (K1) (< 2 μm), (b) FTIR-ATR measurements of selected menilite shale samples (K1) (< 2 μm)

dioctahedral vermiculite formation (e.g. Wilson 1999 and literature cited therein; Churchman and Lowe 2012 and literature cited therein). However, mica-derived dioctahedral vermiculite in soils is always accompanied by different kinds of mica-vermiculite mixed-layered minerals (Skiba 2007, 2013; Skiba et al. 2018). The studied soils did not contain mica-vermiculite minerals, which indicated that dioctahedral vermiculite formed rather at the expense of chlorite than mica.

Formation of vermiculite at the expense of chlorite is a commonly reported process for trioctahedral species (e.g., Adams and Kassim 1983; Argast 1991; Bain 1977; Murakami et al. 1996). In general (e.g., Wilson 1999 and literature cited therein; Churchman and Lowe 2012 and literature cited therein), it is accepted that the vermiculitization of trioctahedral chlorite proceeds via depletion of Fe and Mg and by a slight loss of Al in such a manner that the mineral gradually loses the trioctahedral character and in the end the newly formed vermiculite is partially dioctahedral (Banfield and Murakami 1998; Proust et al. 1986; Środoń 1999; Wilson 2004). This study, however, describes vermiculitization of di-trioctahedral chlorite (sudoite). As indicated by FTIR data (Fig. 8 ((a, b)), vermiculitization of sudoite present in the studied soils was rather straightforward and proceeded due to dissolution and removal of the interlayer trioctahedral sheet. Coexistence of dioctahedral vermiculite with R1 chlorite-vermiculite strongly suggested that vermiculitization

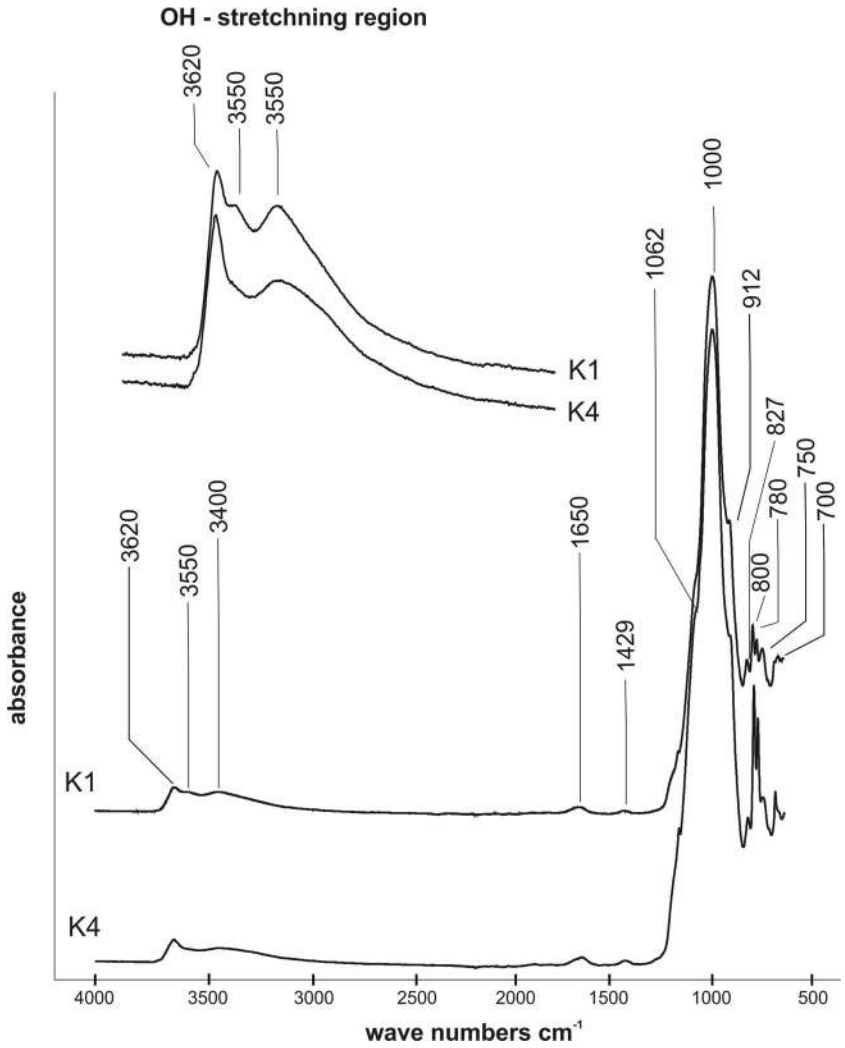


**Fig. 8** (continued)

proceeded via an intermediate stage of chlorite-vermiculite mixed-layered minerals.

Kaolinite was identified in clay fractions from all soil horizons, but no clear depth-distribution trend for the mineral was noted. The traces of kaolinite in the menilite shale K1 profile that appeared to be less-weathered material indicated that kaolinite was not inherited from the menilite shales. Three possible origins of this material have to be considered: (i) transformation of primary clays, (ii) neoformation from soil solutions and (iii) aeolian deposition (Bronger and Bruhn-Lobin 1997; Mavris et al. 2011; Skiba 2007; Waroszewski et al. 2019). According to Dudek et al. (2006), kaolinite may be formed in weathering environments by transformation of dioctahedral smectite due to dissolution of every second tetrahedral sheet. The process leads first to the formation of kaolinite-smectite mixed-layered minerals and eventually to discrete kaolinite. The studied soils did not contain smectite; however, one can imagine the same mechanism of the incongruent dissolution of dioctahedral vermiculite leading to the formation of kaolinite. The fact that the studied soils did not contain kaolinite-vermiculite mixed-layered minerals indicates that transformation is an unlikely mechanism for kaolinite formation in the soils. Neoformation (crystallization from soil solution) of kaolinite in studied soils was likely process responsible for kaolinite presence in the soils. This is indicated by the fact that traces of kaolinite were present in the menilite shale of the K4 profile, which seemed to be quite weathered relative to the material of the K1 profile (Fig. 8 ((a, b). In other words, the fact that kaolinite was present in rock fragments from the K1 profile indicated that at least part of the kaolinite present in the studied soils was definitively not of aeolian origin. However, the aeolian origin of the kaolinite cannot be completely ruled out in this study, as kaolinite was reported from airborne dusts collected in nearby areas (Manecki et al. 1978; Šucha et al. 2001). The aeolian contribution could only be speculated on the basis of the high content of silt fraction from within the whole profiles, at 40 to 60% (fine and coarse silt in total, Fig. 2, Table S1). However, considering the

**Table 5** Major oxides, Hf and Zr content and weathering indices of studied soils

| Soil | Depth | Soil horizon | $SiO_2$ % | $Al_2O_3$ | $Fe_2O_3$ | MgO | CaO | $Na_2O$ | $K_2O$ | Hf ppm | Zr | CIA | ICV |
|---|---|---|---|---|---|---|---|---|---|---|---|---|---|
| K1 | 0–20 | Ap | 55.8 | 16.0 | 6.78 | 1.64 | 0.46 | 0.93 | 2.87 | 4.6 | 135 | 79.0 | 0.85 |
| | 20–33 | AB | 58.8 | 17.1 | 7.15 | 1.65 | 0.41 | 0.93 | 3.00 | 4.8 | 148 | 79.8 | 0.83 |
| | 33–50 | Bt | 61.7 | 16.4 | 7.09 | 1.71 | 0.27 | 0.99 | 2.94 | 5.2 | 136 | 79.7 | 0.85 |
| | 50–70 | 2BtC1 | 58.6 | 18.2 | 7.55 | 1.93 | 0.26 | 0.89 | 3.38 | 4.7 | 150 | 80.1 | 0.82 |
| | 70–110 | 2BtC2 | 60.0 | 17.5 | 7.43 | 1.87 | 0.23 | 0.94 | 3.25 | 5.1 | 144 | 79.9 | 0.84 |
| | > 110 | 2C | 57.9 | 18.6 | 7.69 | 2.00 | 0.26 | 0.87 | 3.46 | 4.5 | 157 | 80.3 | 0.82 |
| K2 | 0–9 | Ah | 51.1 | 16.8 | 6.64 | 1.84 | 0.90 | 0.87 | 3.42 | 4.0 | 152 | 76.5 | 0.86 |
| | 9–25 | Btg1 | 54.0 | 18.5 | 7.27 | 2.07 | 2.50 | 0.86 | 3.73 | 4.2 | 167 | 72.3 | 0.94 |
| | 25–52 | 2Btg2 | 52.6 | 17.4 | 6.93 | 1.92 | 4.61 | 0.90 | 3.55 | 4.1 | 159 | 65.8 | 1.08 |
| | 52–76 | 2BtCg | 50.4 | 16.5 | 6.16 | 2.06 | 7.12 | 0.82 | 3.39 | 3.9 | 156 | 59.4 | 1.23 |
| | 76–105 | 2C | 50.5 | 16.4 | 6.56 | 2.18 | 6.75 | 0.86 | 3.32 | 3.9 | 148 | 60.0 | 1.25 |
| K3 | 0–8 | A | 57.8 | 16.4 | 6.92 | 1.80 | 0.28 | 0.89 | 3.05 | 5.1 | 140 | 79.6 | 0.85 |
| | 8–21 | 2AB | 57.0 | 18.2 | 7.33 | 2.01 | 0.49 | 0.86 | 3.41 | 4.5 | 156 | 79.3 | 0.83 |
| | 21–31 | 2Bt1 | 55.4 | 19.0 | 7.31 | 2.10 | 0.58 | 0.97 | 3.63 | 4.8 | 158 | 78.6 | 0.82 |
| | 31–46 | 2Bt2 | 55.7 | 19.1 | 7.24 | 2.10 | 0.58 | 0.91 | 3.76 | 4.1 | 170 | 78.5 | 0.82 |
| | 46–58 | 3BtC1 | 56.0 | 19.2 | 7.37 | 2.10 | 0.56 | 0.88 | 3.87 | 4.3 | 169 | 78.4 | 0.83 |
| | 58–80 | 3BtC2 | 54.7 | 18.8 | 8.07 | 2.14 | 0.63 | 0.83 | 3.80 | 4.0 | 168 | 78.2 | 0.88 |
| | 80–113 | 3C | 52.3 | 18.4 | 8.12 | 1.98 | 2.47 | 0.81 | 3.73 | 4.1 | 169 | 72.4 | 0.99 |
| K4 | 0–7 | A | 59.9 | 16.5 | 6.38 | 1.66 | 0.13 | 0.91 | 2.90 | 5.6 | 141 | 80.8 | 0.79 |
| | 7–17 | ABt | 59.8 | 17.3 | 6.69 | 1.84 | 0.17 | 0.92 | 3.10 | 5.4 | 146 | 80.5 | 0.80 |
| | 17–36 | Bt1 | 61.1 | 17.0 | 6.64 | 1.86 | 0.27 | 0.97 | 3.09 | 5.6 | 149 | 79.7 | 0.82 |
| | 36–51 | Bt2 | 59.4 | 18.1 | 6.89 | 1.99 | 0.32 | 0.90 | 3.33 | 5.2 | 160 | 79.9 | 0.81 |
| | 51–70 | 2BtC | 56.9 | 19.6 | 7.04 | 2.20 | 0.37 | 0.84 | 3.80 | 4.4 | 166 | 79.6 | 0.78 |
| | 70–90 | 2C | 56.9 | 19.6 | 7.04 | 2.20 | 0.37 | 0.84 | 3.80 | 4.4 | 162 | 79.6 | 0.78 |

relatively low content of Zf and Hf, which are widely considered as the indices of silt admixture (Galović and Peh 2014; Scheib and Lee 2010; Scheib et al. 2014; Waroszewski et al. 2018a, 2018b), it can only be stated that aeolian admixture was absent or only present in small amounts in the studied soils.

On the other hand, the uniform distribution of kaolinite in the investigated soil horizons indicated that kaolinite might be crystallized from percolating soil solutions, rich in Al and Si, similarly to cases described in other studies (Dere et al. 2016; Dixon 1989; Skiba 2007). It is worth noting that in the studied soils, kaolinite appeared to be formed both in acidic and alkaline conditions. This finding is in good agreement with data from the literature, as kaolinite formation in soils of temperate climates was described both for acidic (Skiba 2007) and alkaline (Skoneczna et al. 2019) soil environments.

R1 illite-smectite identified in all studied soils is most likely a product of transformation (smectitization) of inherited illite. This was indicated by the fact that in all studied soil profiles, an increase in the amount of R1 illite-smectite relative to the amount of illite was observed towards the top of the profiles (Fig. 7). This finding is generally in good agreement with literature data (e.g. Wilson 1999 and literature cited therein; Churchman and Lowe 2012 and literature cited therein), as formation of smectite at the expense of illite is always considered as one of the major weathering process in soils. However, in most of the studies, mica interlayers are first transformed into vermiculite interlayers and then afterwards into smectite. In the case of the studied soils, smectite appeared to be formed directly from illite. However, it is worth noting here that the smectitic character of expanding interlayers in the mica-containing mixed-layered minerals was recognized in the present study using a glycerol test, which, according to Malla and Douglas (1987), overestimates soil smectites and underestimates soil vermiculites. To recognize the actual character of the expanding interlayers, one would have to measure the layer charge. In the case of the studied materials, this was not possible because the mixed-layered minerals were accompanied by vermiculite.

## 5.2 Influence of calcium carbonate on clay mineral transformations

The studied soils, developed from menilite shale slope deposits, showed stratification within each soil profile (Fig. 2), yet some morphological features suggest that the soil profiles

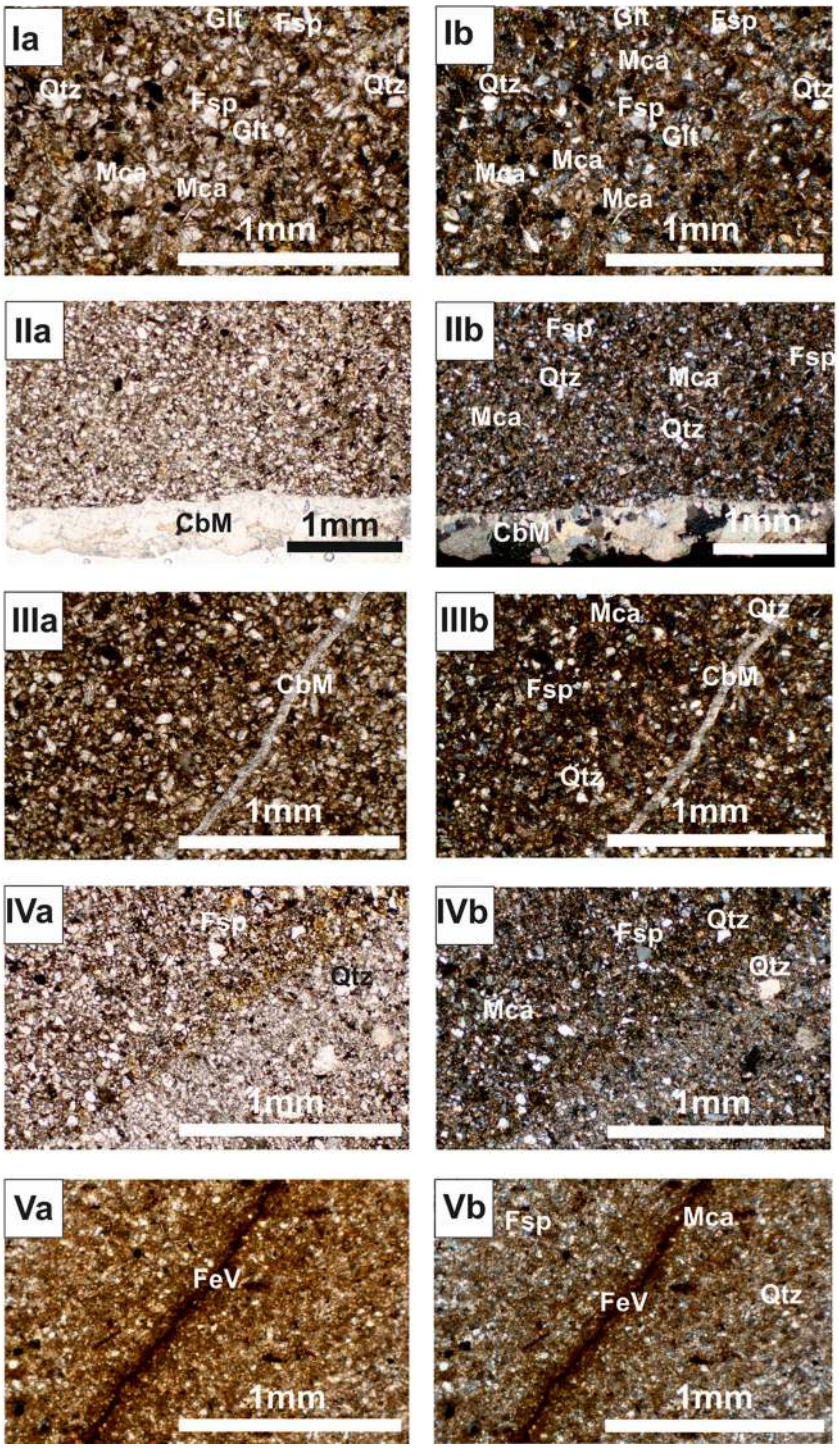


**Fig. 9** Microphotographs of menilite shale thin sections from the studied soil profiles. (Ia, Ib, K1): Qtz quartz, Fsp feldspar, Mca mica. (IIa, IIb, K1): Qtz quartz, Fsp feldspar, Mca mica, CbM carbonate minerals. (IIIa, IIIb, K2): Qtz quartz, Mca mica, CbM carbonate minerals. (IVa, IVb, K3): Qtz quartz, Fsp feldspar, Mca mica (Va, Vb, K4): FeV ferruginous vein, Mca mica, Qtz quartz. Bar length = 1 mm. Ia, IIa, IIIa, IVa, Va—PPL microphotographs, Ib, IIb, IIIb, IVb, Vb—XPL microphotographs

were influenced by different slope processes. Profile K1 could be the part of deep colluvial cover which was probably formed under slope washing processes (Guerra et al. 2017), which can be concluded based on its location (the lower part of the slope, Figs. 1 and 7) and low content and homogeneous distribution of coarse fragment in the soil profile (Table 3). By contrast, in the soils K2, K3 and K4, colluvial material was accumulated on coarse-grained slope deposits with features of short-range transport (Fig. 7) such as rock fragments, whose orientation is probably due to solifluction or creeping process (Schaetzl and Anderson 2005; Waroszewski et al. 2013).

The soils were characterized by various content of primary calcium carbonate (see the Method section, Table 3). It would seem that in soils where calcium carbonate has been partially (profiles K1 and K3) and completely (K4) under the leaching process in the past, or the carbonate removal have not started

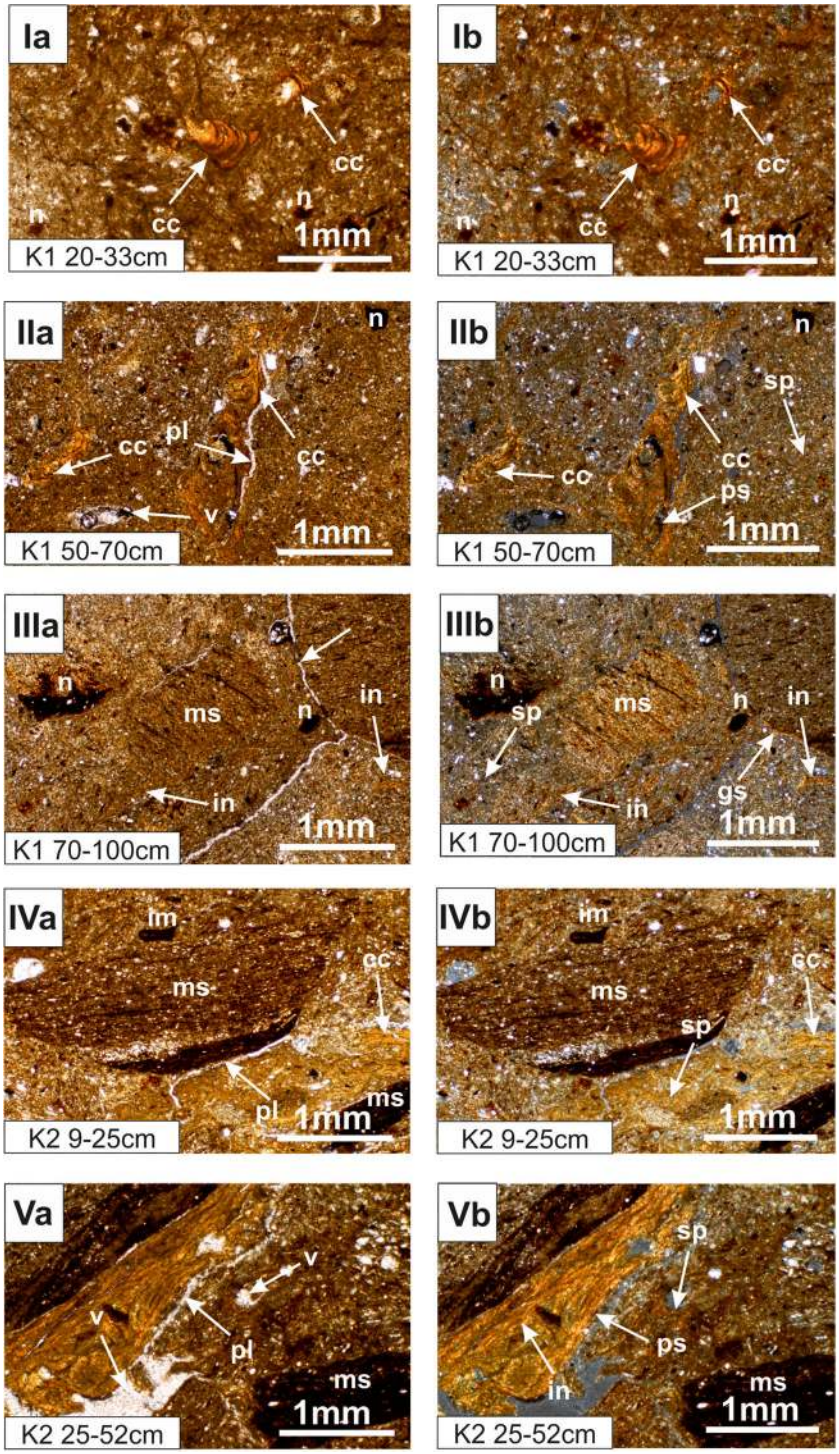


**Fig. 10** (a) Microphotographs of soil thin sections from studied profiles. (Ia, Ib): (cc) crescent clay coating, (n) iron-manganese nodule; (IIa, IIb): (cc) crescent clay coating, (n) iron-manganese nodule, (v) vughs type of voids, (pl) planar type of voids, (sp) speckled b-fabric, (ps) porostriated b-fabric; (IIIa, IIIb): (n) iron-manganese nodule; (in) infillings of illuvial clay, (ms) weathered menilite shale, (pl) planar type of voids, (ps) porostriated b-fabric, (gs) granostriated b-fabric; (IVa, IVb): (in) infillings of illuvial clay, (ms) weathered menilite shale, (cc) crescent clay coating, (pl) planar type of voids, (ps) porostriated b-fabric, (im) iron-manganese impregnation; (Va, Vb): (pl) planar type of voids, (v) vughs type of voids, (in) infillings of illuvial clay, (ps) porostriated b-fabric, (sp) speckled b-fabric. Bar length = 1 mm. Ia, IIa, IIIa, IVa, Va—PPL microphotographs, Ib, IIb, IIIb, IVb, Vb—XPL microphotographs, (b) Microphotographs of soil thin sections from studied profiles. (Ia, Ib): (ms) weathered menilite shale, (in) infillings of illuvial clay, (gs) granostriated b-fabric, (ps) porostriated b-fabric; (IIa, IIb): (im) iron-manganese impregnation, (in) infillings of illuvial clay; (IIIa, IIIb): (v) vughs type of voids, (pl) planar type of voids, (in) infillings of illuvial clay, (im) iron-manganese impregnation; (IVa, IVb): (n) iron-manganese nodule, (im) iron-manganese impregnation; (Va, Vb): (v) vughs type of voids, (pl) planar type of voids, (ms) weathered menilite shale, (cc) crescent clay coating, (ps) porostriated b-fabric, (gs) granostriated b-fabric. Bar length = 1 mm. Ia, IIa, IIIa, IVa, Va—PPL microphotographs, Ib, IIb, IIIb, IVb, Vb—XPL microphotographs

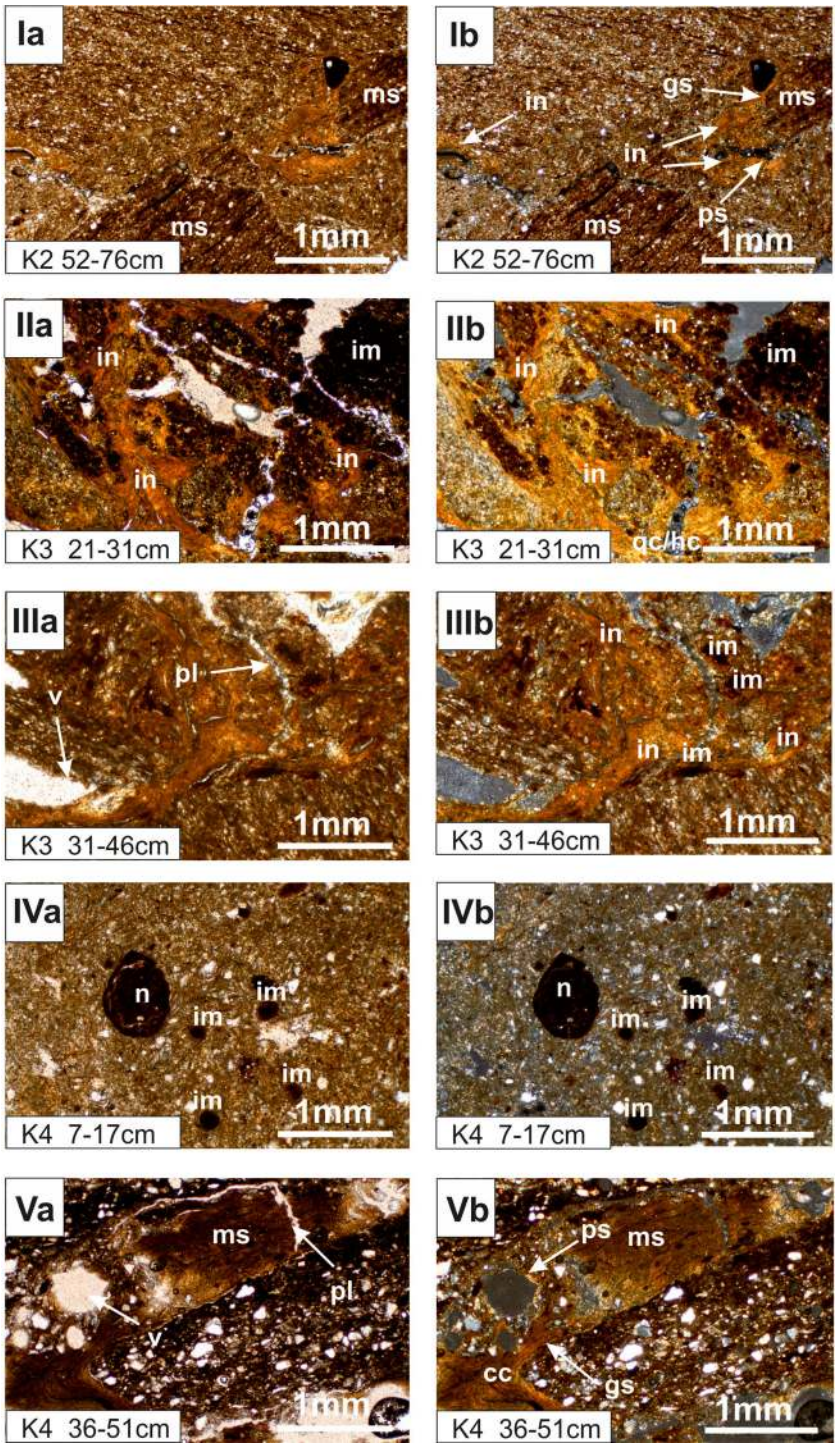


**Fig. 10** (continued)

yet (K2), the mineralogical composition of clay fraction would be diversified both between the analysed soil profiles and between the horizons. However, despite the fact that different slope processes shaped parent material before formation of soil and different patterns of calcium carbonate distribution were recognized, the studied soils were characterized by high similarity in terms of clay mineral composition and paths of their transformations (Figs. 3 ((a, b), 4 and 7). Consequently, it was noted that in the studied soils, the path of clay minerals transformation was not influenced by leaching of calcium carbonate. Additionally, it seems that relocated material on slopes, providing substrate for soils and clay transformation, has no direct impact on mineralogical composition of clay fraction.

The obtained results are in contradiction to the data presented by other authors concerning clay mineralogy in soils derived from slope deposits rich in calcium carbonates. For example, the study by Kacprzak and Derkowski (2007) on Eutric Cambisols from the Pieniny Mountains in South Poland reported that, together with the leaching of calcium carbonate out of soil profiles, changes of direction in clay minerals transformation could be recognized. At the same time, Drewnik et al. (2014) analysed clay mineral composition in two loess soils, the first one non-carbonate and the second one rich in calcium carbonate, and furthermore stated the differences in clay mineralogy. Subsequent results suggest that clay mineral dispersion and transformation is possible after decalcification of carbonate soil horizons that is accompanied by a decrease in soil pH values. Simultaneously, in soil horizons where the dissolution and leaching of carbonates occurs, the more intense weathering of silicates layers should be noted. At the same time, under similar soil conditions in studied Kacwin soils, the non-carbonate horizons (or horizons where a low calcium carbonate content is indicated) should indicate a higher degree of clay minerals transformation, while the more calcium carbonate-rich horizons should point to stabilization of phyllosilicates. However, in view of the results of the present study, such assumptions apparently do not hold for the soil developed from the slope cover, which has been repeatedly redeposited in the past.

It seems that uniform composition of clay minerals was the result of the initial stage of soil development. The slope cover that originally consisted of the parent material for Kacwin's soils was subjected to mass movements—probably at the same time and with the same intensity—which finally lead to homogenization of soil material and homogenization of the mineralogy of the clay fraction. Additionally, the pedogenesis could have proceeded on the same scale within all studied soils.

This assumption seems to be correct, considering the degree of weathering process within the slope deposits. To assess the degree of weathering process, two indices—the CIA and ICV—have been calculated (Table 5; Böhlert et al. 2011; Depetris et al. 2014; Nesbitt and Young 1982). The values of the CIA and ICV indices ranged from 60.0 to 80.8 and from 0.78 to 1.25 respectively (Table 5) and indicated the high chemical alternation and maturity of the soil (Pasquini et al. 2017), which gave rise to micromorphological features related to high weathering transformation of coarse fragments, as visible on thin sections (Fig. 10 (a): IIIa, IIIb, IVa, IVb; Fig. 10 (b): Ia, Ib, Va, Vb). Furthermore, the indices' values were distributed randomly, and did not evidence depth-dependent continuous weathering of the soils (Table 5), suggesting that soil material was under redeposition processes acting along the slope (Loba et al. 2020; Pasquini et al. 2017). Nevertheless, when considering the homogeneous geochemical data (Table 5) that soil material enhanced by slope processes could proceed on a small scale was also reflected in the similar state of clays transformation. Alternatively, the studied soil material might be mixed on the slope to a great extent, further hampering clay minerals transformation and contributing to their high homogeneous composition.

Additionally, the illuviation process may have had a great influence here. According to the literature, the composition of clay minerals might be controlled by material translocation down the soil profile through a clay illuviation (lessivage) process (e.g. Skiba et al. 2014). However, based on the morphological and micromorphological properties of the studied soils (Table 3, Table S2), it seems to be very likely that the lessivage process did not affect the Kacwin soils in the traditional way. For instance, in the studied profiles, the translocation of clay material was not particularly intense and it had a very weak short-range character; therefore, no clear argic horizons could be developed, which would result in concentration of finer clays only in the Bt horizon. In addition, in this study, there is no clear evidence that some horizons have been depleted in clay; the traces of clay translocation were observed not only in the Bt horizon but also within other horizons in various forms, such as clay coatings or infillings of illuvial clay (Fig. 10 (a, b), Table S2, Bonifacio et al. 2009; Kitagawa 2005; Waroszewski et al. 2019). The character of such a lessivage process could not have influenced the clear differences in mineralogy of clay fraction, but might contribute to the uniformity of the phyllosilicates composition.

## 6 Conclusions

In this study, calcium carbonate did not influence the composition and transformation of clay minerals. Despite the fact that soils were characterized by different content and distribution of calcium carbonate within the solum and additionally indicated various morphological features, the mineralogical composition of clay fraction was very uniform.

Among the recognized phyllosilicates, chlorite and illite present in the studied soils were inherited from parent menilite shales. Dioctahedral vermiculite identified in all the soil horizons was most likely formed by transformation of inherited chlorite by dissolution of the trioctahedral interlayer sheet. The transformation proceeded via chlorite-vermiculite mixed-layer phases. R1 illite-smectite mixed-layered minerals appeared to be products of transformation (i.e. smectitization) of inherited illite. The smectite interlayers seemed to be formed directly from illite without formation of vermiculite precursors. Kaolinite was likely neoformed in the studied soils in both acidic and alkaline soil horizons. The occurrence of kaolinite seemed to also be partially connected with aeolian origin.

The uniform composition of the clay minerals suggested that mass movement which controlled the formation of slope covers had a similar character and intensity across the whole

of the slope. Furthermore, it seems that the pedogenesis of all soils proceeded on the same scale of advancement. This was stated through similar values of weathering indices (CIA and ICV) and lack of depth-dependent continuous weathering of the soils. Moreover, weak intensity of the illuviation process within the homogeneous substrate could have resulted in the very homogeneous composition of clay minerals in the studied soils.

**Acknowledgements** The authors are indebted to the reviewers for their constructive remarks and comments on an earlier version of the manuscript as well as to Jarosław Waroszewski, Ph.D. for his help in classification of the studied soils in terms of Soil Taxonomy (Soil Survey Staff 2014).

**Funding** This research was financed by the National Science Centre (Poland) (PRELUDIUM 14 project no. 2017/27/N/ST10/00342) and Ministry of Science and Higher Education of the Republic of Poland, No. BM–4112/17 and BM–2120/18.

## Compliance with ethical standards

**Conflict of interest** The authors declare that they have no conflicts of interest.



## References

Adams WA, Kassim JK (1983) The origin of vermiculite in soils developed from Lower Palaeozoic sedimentary rocks in Mid-Wales. Soil Sci Soc Am J 47:316–320

Ajami M, Heidari A, Khormali F, Gorji M, Ayoubi S (2018) Effects of environmental factors on classification of loess derived soils and clay minerals variations, northern Iran. J Mt Sci 15:976–991. https://doi.org/10.1007/s11629-017-4796-y

Ahlrichs JL, Fraser AR, Russell JD (1972) Interaction of ammonia with vermiculite. Clay Miner 9:263–273

Argast S (1991) Chlorite vermiculization and pyroxene etching in an aeolian periglacial sand dune, Allen county, Indiana. Clay Clay Miner 39:622–633

Bain DC (1977) The weathering of ferruginous chlorite in a podzol from Argyllshire, Scotland. Geoderma 17:193–208

Banfield JF, Murakami T (1998) Atomic resolution transmission electron microscope evidence for the mechanism by which chlorite weathers to 1:1 semiregular chlorite vermiculite. Am Mineral 83:348–357

Barton CD, Karathanasis AD (2002) Clay minerals, clay minerals. In: Lal, R. (Ed.), Encyclopedia of soil science. Marcel Dekker, New York, USA, 187–192. doi:https://doi.org/10.1081/E-ESS-120001688

Böhlert R, Mirabella A, Plötze M, Egli M (2011) Landscape evolution in Val Mulix, eastern Swiss Alps—soil chemical and mineralogical analyses as age proxies. Catena 87:313–325

Bonifacio E, Falsone G, Simonov G, Sokolova T, Tolpeshta I (2009) Pedogenic processes and clay transformations in besequal soils of the southern Taiga zone. Geoderma 149:66–75

Bronger A, Bruhn-Lobin N (1997) Paleopedology of Terrae rossae-Rhodoxeralfs from quaternary calcarenites in NW Morocco. Catena 28: 279–295. doi:https://doi.org/10.1016/S0341-8162(96)00043-475-86. doi:https://doi.org/10.1016/j.geoderma.2014.11.004

Brown G, Brindley GW (1984) Crystal structures of clay minerals and their X-ray identification, 2nd edn. Mineralogical Society, London, pp 305–360

Carnicelli S, Mirabella A, Cecchini G, Sanesi G (1997) Weathering of chlorite to a low-charge expandable mineral in a spodosol on the Apennine Mountains, Italy. Clay Clay Miner 45:28–41

Churchman GJ, Lowe DJ (2012) Alteration, formation and occurrence of minerals in soils. In: Huang, P.M.; Li, Y; Sumner, M.E. (editors) "Handbook of Soil Sciences. 2ndedition. Vol. 1: Properties and Processes". CRC Press (Taylor & Francis),Boca Raton, FL, 20.1–20.72

Costantini EAC, Damiani D (2004) Clay minerals and the development of quaternary soils in central Italy. Rev Mex Ciencias Geol 21:144–159

Cox R, Lowe DR, Cullers RL (1995) The influence of sediment recycling and basement composition on evolution of mudrock chemistry in the southwestern United States. Geochim Cosmochim Acta 59(14): 2919–2940

Delijska A, Blazheva T, Petkova L, Dimov L (1988) Fusion with lithium borate as sample preparation for ICP and AAS analysis. Fresenius' Zeitschrift für Anal Chemie 332:362–365. https://doi.org/10.1007/BF00468816

Depetris PJ, Pasquini AI, Lecomte KL (2014) Weathering and the riverine denudation of continents. Springer, Berlin 95

Dere AL, White TS, April RH, Brantley SL (2016) Mineralogical transformations and soil development in shale across a latitudinal climosequence. Soil Sci Soc Am J 80(3):623–636

Dixon JB (1989) Kaolin and serpentine group minerals. In: Dixon JB, Weed SB (eds) Minerals in soil environments, SSSA Book Series, vol 1, 2nd edn, pp 476–525

Drewnik M, Skiba M, Szymański W, Zyła M (2014) Mineral composition vs. soil forming processes in loess soils—a case study from Kraków (southern Poland). Catena 119:166–173. https://doi.org/10.1016/j.catena.2014.02.012

Dudek T, Cuadros J, Fiore S (2006) Interstratified kaolinite-smectite: nature of the layers and mechanism of smectite kaolinization. Am Mineral 91(1):159–170. https://doi.org/10.2138/am.2006.1897

Eberl DD, Farmer VC, Barrer RM (1984) Clay mineral formation and transformation in rocks and soils. Philos Trans R Soc A Math Phys Eng Sci 311(1517):255–257. https://doi.org/10.1098/rsta.1984.0026

Egli M, Mirabella A, Fitze P (2001) Clay mineral formation in soils of two different chronosequences in the Swiss Alps. Geoderma 104: 145–175. https://doi.org/10.1016/S0016-7061(01)00079-9

Egli M, Zanelli R, Kahr G, Mirabella A, Fitze P (2002) Soil evolution and development of the clay mineral assemblages of a Podzol and a Cambisol in 'Meggerwald', Switzerland. Clay Miner 37(2):351–366. https://doi.org/10.1180/0009855023720039

Egli M, Mirabella A, Sartori G, Giaccai D, Zanelli R, Plötze M (2007) Effect of slope aspect on transformation of clay minerals in Alpine soils. Clay Miner 42:373–398

Egli M, Mirabella A, Sartori G (2008) The role of climate and vegetation in weathering and clay mineral formation in late Quaternary soils of

the Swiss and Italian Alps. Geomorphology 102:307–324. https://doi.org/10.1016/j.geomorph.2008.04.001

Emadi M, Baghernejad M, Memarian H, Saffari M, Fathi H (2008) Genesis and clay mineralogical investigation of highly calcareous soils in semi-arid regions of Southern Iran. J Appl Sci 8:288–294. https://doi.org/10.3923/jas.2008.288.294

FAO (Food and Agricultural Organization of the United Nations) (2006) Guidelines for soil description, fourth edition. Food and Agriculture Organization of the United Nations. Rome IT EU, 97 p

Ferreira EP, dos Anjos LHC, Pereira MG, Valladares GS, Cipriano-Silva R, de Azevedo AC (2016) Genesis and classification of soils containing carbonate on the Apodi Plateau, Brazil. Revista Brasileira de Ciência Do Solo, 40 (October). https://doi.org/10.1590/18069657rbcs20150036

Fiantis D, Nelson M, Shamshuddin J, Goh TB, Van Ranst E (2010) Determination of the geochemical weathering indices and trace elements content of new volcanic ash deposits from Mt. Talang (West Sumatra) Indonesia. Eurasian Soil Sci 43:1477–1485. https://doi.org/10.1134/s1064229310130077

Galović L, Peh Z (2014) Eolian contribution to geochemical and mineralogical characteristics of some soil types in Medvednica Mountain, Croatia. Catena 117:145–156

Goldberg K, Humayun M (2010) The applicability of the chemical index of alteration as a paleoclimatic indicator: an example from the Permian of the Paraná Basin, Brazil. Palaeogeogr Palaeoclimatol Palaeoecol 293: 175–183. https://doi.org/10.1016/j.palaeo.2010.05.015

Guerra AJT, Fullen MA, do CO JM, JFR B, Shokr MS (2017) Slope processes, mass movement and soil erosion: a review. Pedosphere 27(1):27–41. https://doi.org/10.1016/S1002-0160(17)60294-7

IUSS Working Group WRB (2015) World Reference Base for Soil Resources 2014, update 2015. International soil classification system for naming soils and creating legends for soil maps. World Soil Resources Reports No. 106. FAO, Rome, 182

Kacprzak A, Derkowski A (2007) Cambisols developed from cover-beds in the Pieniny Mts. (southern Poland) and their mineral composition. Catena 71:292–297. https://doi.org/10.1016/j.catena.2007.01.004

Khormali F, Abtahi A (2003) Origin and distribution of clay minerals in calcareous arid and semi-arid soils of Fars Province, southern Iran. Clay Miner 38:511–527. https://doi.org/10.1180/0009855023740112

Kitagawa Y (2005) Characteristics of clay minerals in Podzols and Podzolic soils. Soil Sci Plant Nutr 51:151–158. https://doi.org/10.1111/j.1747-0765.2005.tb00020.x

Kowalska J, Skiba M, Maj-Szeliga K, Mazurek R, Zaleski T (2020) The properties of calcium carbonate-rich soils from Kacwin village (South Poland). [Dataset]. Zenodo. doi:https://doi.org/10.5281/zenodo.3972136, Website: https://zenodo.org/record/3972136#.XymDmIgzbIU

Kulka A, Rączkowski W, Żytko K, Gucik S, Paul Z (1985) Szczegółowa mapa geologiczna Polski w skali 1:50 000, arkusz 1050: Szczawnica-Krościenko. Wydawnictwo Geologiczne, Warszawa (in Polish)

Küfmann C (2008) Are Cambisols in Alpine Karst autochthonous or Eolian in origin. Arctic Antarct Alp Res 40:506–518

Loba A, Sykuła M, Kierczak J, Łabaz B, Bogacz A, Waroszewski J (2020) In situ weathering of rocks or aeolian silt deposition: key parameters for verifying parent material and pedogenesis in the Opawskie Mountains—a case study from SW Poland. J Soils Sediments 20(1):435–451

Malla PB, Douglas LA (1987) Identification of expanding layer silicates: layer charge vs expansion properties: in Proc. Intern. Clay Conf., Denver, 1985, L. G. Schultz, H. van Olphen, and F. A. Mumpton, (ed), The Clay Minerals Society, Bloomington, Indiana 277–283

Manecki A, Michalik M, Obidowicz A,Wilczyńska-Michalik W (1978) Charakterystyka mineralogiczna i palinologiczna pyłów eolicznych z opadów w Tatrachw latach 1973 i 1974. Pr Mineral 57: 19–60 (in Polish)

Mavris C, Plötze M, Mirabella A, Giaccai D, Valboa G, Egli M (2011) Clay mineral evolution along a soil chronosequence in an Alpine proglacial area. Geoderma 165:106–117

Mehra OP, Jackson ML (1960) Iron oxide removal from soils and clays by a dithionite citrate system buffered with sodium bicarbonate. Proc. 7th Int. Conf. Clays and clay minerals, Pergamon press, London, 317–327

Méring J (1949) L'Intéreference des Rayons X dans les systems à stratification dé sordonnée: Acta Crystallogr 2: 371–77

Moore DM, Reynolds RC (1997) X-ray diffraction and the identification and analysis of clay minerals. 2nd ed. Oxford Univ. Press, New York

Munsell (1975) Standard Soil Color Charts

Murakami T, Isobe H, Sato T, Ohnuki T (1996) Weathering of chlorite in a quartz-chlorite schist. I. Mineralogical and chemical changes. Clay Clay Miner 44:244–256

Mystkowski K (1999) ClayLab, a computer program for processing and interpretation of X-ray diffractograms of clays. Conference of European Clay Groups Association, EUROCLAY, 114–115. Krakow, Poland

Nesbitt HW, Young GM (1982) Early Proterozoic climates and plate motions inferred from major element chemistry of lutites. Nature 299(5885):715–717

Oliveira DP, Sartor LR, Souza Júnior VS, Corrêa MM, Romero RE, Andrade GRP, Ferreira TO (2018) Weathering and clay formation in semi-arid calcareous soils from Northeastern Brazil. Catena 162: 325–332. https://doi.org/10.1016/j.catena.2017.10.030

Otrębska-Starklowa B, Hess M, Olecki Z, Trepińska J, Kowanetz L (1995) Klimat. In: Warszyńska J. (ed), Karpaty Polskie. Uniwersytet Jagielloński, 31–48 (in Polish)

Pal DK, Srivastava P, Bhattacharyya T (2003) Clay illuviation in calcareous soils of the semiarid part of the Indo-Gangetic Plains, India. Geoderma 115(3–4):177–192. https://doi.org/10.1016/S0016-7061(02)00377-4

Pasquini AI, Campodonico VA, Rouzaut S, Giampaoli V (2017) Geochemistry of a soil catena developed from loess deposits in a semiarid environment, Sierra Chica de Córdoba, central Argentina. Geoderma 295:53–68. https://doi.org/10.1016/j.geoderma.2017.01.033

Proust D, Eymery JD, Beaufort D (1986) Supergene vermiculitization of a magnesian chlorite; iron and magnesium removal processes. Clay Clay Miner 34:572–580

Rate AW, Sheikh-Abdullah SM (2017) The geochemistry of calcareous forest soils in Sulaimani Governorate, Kurdistan region, Iraq. Geoderma 289:54–65. https://doi.org/10.1016/j.geoderma.2016.11.028

Righi D, Huber K, Keller C (1999) Clay formation and podzol development from postglacial moraines in Switzerland. Clay Miner 34:319–332

Russell JD, Fraser AR (1994) Infrared methods. In: Wilson MJ (ed) Clay mineralogy: spectroscopic and chemical determinative methods. Chapman & Hall, London, pp 11–67

Schaetzl R, Anderson S (2005) Soils, genesis and geomorphology. Cambridge University Press, Cambridge 817

Scheib AJ, Birke M, Dinelli E, GEMAS Project Team (2014) Geochemical evidence of aeolian deposits in European soils. Boreas 43:175–192

Scheib AJ, Lee J (2010) Mapping Late Pleistocene and Holocene aeolian sediments in East Anglia, UK: the application of regionalscale geochemical data. Quaternary Newsletter 120:5–14

Skiba M (2007) Clay mineral formation during podzolization in an Alpine environment of the Tatra Mountains, Poland. Clay Clay Miner 55:618–634. https://doi.org/10.1346/CCMN.2007.0550609

Skiba M, Szczerba M, Skiba S, Bish DL, Grybos M (2011) The nature of interlayering in clays from a podzol (Spodosol) from the Tatra

Mountains, Poland. Geoderma 160:425–433. https://doi.org/10.1016/j.geoderma.2010.10.013
Skiba M (2013) Evolution of dioctahedral vermiculite in geological environments—an experimental approach. Clay Clay Miner 61(3–4):290–302
Skiba M, Maj-Szeliga K, Szymański W, Błachowski A (2014) Weathering of glauconite in soils of temperate climate as exemplified by a Luvisol profile from Góra Puławska, Poland. Geoderma 235–236:212–226
Skiba M, Skiba S, Derkowski A, Maj-Szeliga K, Dziubińska K (2018) Formation of $NH^4$-illite-like phase at the expense of dioctahedral vermiculite in soil and diagenetic environments—an experimental approach. Clay Clay Miner 66(7):74–85
Skiba S (1995) Pokrywa glebowa. In: Warszyńska J. (Eds.), Karpaty Polskie. Uniwersytet Jagielloński, 69–76 (in Polish)
Skoneczna M, Skiba M, Szymański W, Kisiel M, Maj-Szeliga K, Błachowski A (2019) Geoderma Weathering of glauconite in alkaline soils of temperate climate : A case study from Górniki , eastern Poland. Geoderma 340:146–156. https://doi.org/10.1016/j.geoderma.2018.12.029
Soil Survey Staff (2010) Keys to soil taxonomy, 11th edn. USDA-NRCS, Washington DC
Soil Survey Staff (2014) Keys to soil taxonomy, Twelfth edn. United States Department of Agriculture, Natural Resources Conservation Service, Lincoln NE USA, 372 p
Stone M, Wild A (1978) The reaction of ammonia with vermiculite and hydrobiotite. Clay Miner 13:337–350
Stoops G (2003) Guidelines for analysis and description of soil and regolith thin sections. Soil Science Society of America, Inc. Madison, Wisconsin, USA, 184
Środon J, Eberl DD (1980) The presentation of X-ray data for clay minerals. Clay Miner 15:317–320
Środoń J (1999) Nature of mi ed-layer clays and mechanisms of their formation and alteration. Annu Rev Earth Planet Sci 27:19–53
Środoń J, Drits VA, McCarty DK, Hsieh JCC, Eberl DD (2001) Quantitative X-ray diffraction analysis of clay-bearing rocks from random preparations. Clay Clay Miner 49:514–528
Środoń J (2006) Identification and quantitative analysis of clay minerals. In: Bergaya F, Theng BKG, Lagaly G (eds) Handbook of clay science. Elsevier, Developments in Clay Science I, pp 773–795
Šucha V, Širáňová V (1991) Potassium and ammonium fixation in smectites by wetting and drying. Clay Clay Miner 39:556–559
Šucha V, Środoń J, Clauer N, Elsass F, Eberl DD, Kraus I, Madejová J (2001) Weathering of smectite and illite–smectite under temperate climatic conditions. Clay Miner 36:403–419
Szymański W, Skiba M, Błachowski A (2017) Influence of redox processes on clay mineral transformation in Retisols in the Carpathian Foothills in Poland. Is a ferrolysis process present? J Soils Sediments 17:453–470. https://doi.org/10.1007/s11368-016-1531-1
Towpasz K, Zemanek B (1995) Szata Roślinna. In: Warszyńska J. (ed), Karpaty Polskie. Uniwersytet Jagielloński, 77–94 (in Polish)
Uzarowicz Ł, Skiba S (2011) Technogenic soils developed on mine spoils containing iron sulphides: mineral transformations as an indicator of pedogenesis. Geoderma 163(1–2):95–108
Waroszewski J, Kalinski K, Malkiewicz M, Mazurek R, Kozlowski G, Kabala C (2013) Pleistocene-Holocene cover-beds on granite regolith as parent material for Podzols—an example from the Sudeten Mountains. Catena 104:161–173. https://doi.org/10.1016/j.catena.2012.11.006
Waroszewski J, Egli M, Kabala C, Kierczak J, Brandova D (2016) Mass fluxes and clay mineral formation in soils developed on slope deposits of the Kowarski Grzbiet (Karkonosze Mountains, Czech Republic/Poland). Geoderma 264:363–378. https://doi.org/10.1016/j.geoderma.2015.08.044
Waroszewski J, Egli M, Brandová D, Christl M, Kabala C, Malkiewicz M, Kierczak J, Glina B, Jezierski P (2018a) Identifying slope processes over time and their imprint in soils of medium-high mountains of Central Europe (the Karkonosze Mountains, Poland). Earth Surf Process Landf 43(6):1195–1212. https://doi.org/10.1002/esp.4305
Waroszewski J, Sprafke T, Kabala C, Musztyfaga E, Łabaz B, Woźniczka P (2018b) Aeolian silt contribution to soils on mountain slopes (Mt. Ślęża, southwest Poland). Quat Res 89(3):702–717. https://doi.org/10.1017/qua.2017.76
Waroszewski J, Sprafke T, Kabała C, Kobierski M, Kierczak J, Musztyfaga E, Loba A, Mazurek R, Łabaz B (2019) Tracking textural, mineralogical and geochemical signatures in soils developed from basalt-derived materials covered with loess sediments (SW Poland). Geoderma 337:983–997. https://doi.org/10.1016/j.geoderma.2018.11.008
Wilson MJ (1999) The origin and formation of clay minerals in soils: past, present and future perspectives. Clay Miner 34:7–25
Wilson MJ (2004) Weathering of the primary rock-forming minerals: processes, products and rates. Clay Miner 39:233–266
Van Reeuwijk LP (2002) Procedures for soil analysis, 6th edn. ISRIC, Wageningen
Velde B, Meunier A (2011) The origin of clay minerals in soils and weathered rocks. Springer-Verlag, Berlin, Heidelberg, 406
Vicente MA, Razzaghe M, Robert M (1977) Formation of aluminium hydroxy vermiculite (intergrade) and smectite from mica under acidic conditions. Clay Miner 12:101–112
Yu Z, Norman MD, Robinson P (2003) Major and trace element analysis of silicate rocks by XRF and laser ablation ICP-MS using lithium borate fused glasses: matrix effects, instrument response and results for international reference materials. Geostand Newslett 27:67–89. https://doi.org/10.1111/j.1751-908X.2003.tb00713.x
Yousefifard M, Ayoubi S, Poch RM, Jalalian A, Khademi H, Khormali F (2015) Clay transformation and pedogenic calcite formation on a lithosequence of igneous rocks in northwestern Iran. Catena 133:186–197. https://doi.org/10.1016/j.catena.2015.05.014
Zagórski Z (2010) Clay minerals as indicators of the soil substrate origin of Rendzinas ( Rendzic Leptosols ) from the Małopolska Upland ( S Poland ). World 19th World Congress of Soil Science, Soil Solutions for a Changing World 1–6 August 2010, Brisbane, Australia
Zhang Y, de Vries W, Thomas BW, Hao X, Shi X (2017) Impacts of long-term nitrogen fertilization on acid buffering rates and mechanisms of a slightly calcareous clay soil. Geoderma 305:92–99. https://doi.org/10.1016/j.geoderma.2017.05.021